Connecting Scales in High-Mass Star and Cluster Formation

Roberto Galván-Madrid

Instituto de Radioastronomía y Astrofísica (IRyA)
UNAM Campus Morelia

A lot of work presented here has been done by:
Andrés F. Izquierdo (U de Antioquia ⇒ Manchester)
Luke Maud (Leiden)
Hauyu Baobab Liu (ESO-Garching)
Yuxin Lin (MPIfR, Bonn)
Manuel Zamora-Avilés (IRyA-UNAM)
Adam Ginsburg (NRAO)

Trancing the Flow, Windermere, UK
03.07.2018

THE SCALES OF STAR FORMATION

What is the interplay between the scales of star (cluster) formation?
$>$ 12 order of magnitude dynamic range in scales!
Gas: Galaxies (10^4 pc) $\leftrightarrow$ GMCs ($10^1 - 10^2$ pc) $\leftrightarrow$ Clumps (10^0 pc) $\leftrightarrow$ Cores (10^{-1} pc) $\leftrightarrow$ Disks (10^{-3} pc) $\leftrightarrow$ Magnetospheres (10^{-7} pc) $\leftrightarrow$ Protoplanets (10^{-8} pc).

Stars: Galaxies $\leftrightarrow$ Star clusters/associations $\leftrightarrow$ Stellar associations/groups $\leftrightarrow$ Stellar systems/stars $\leftrightarrow$ Planets.

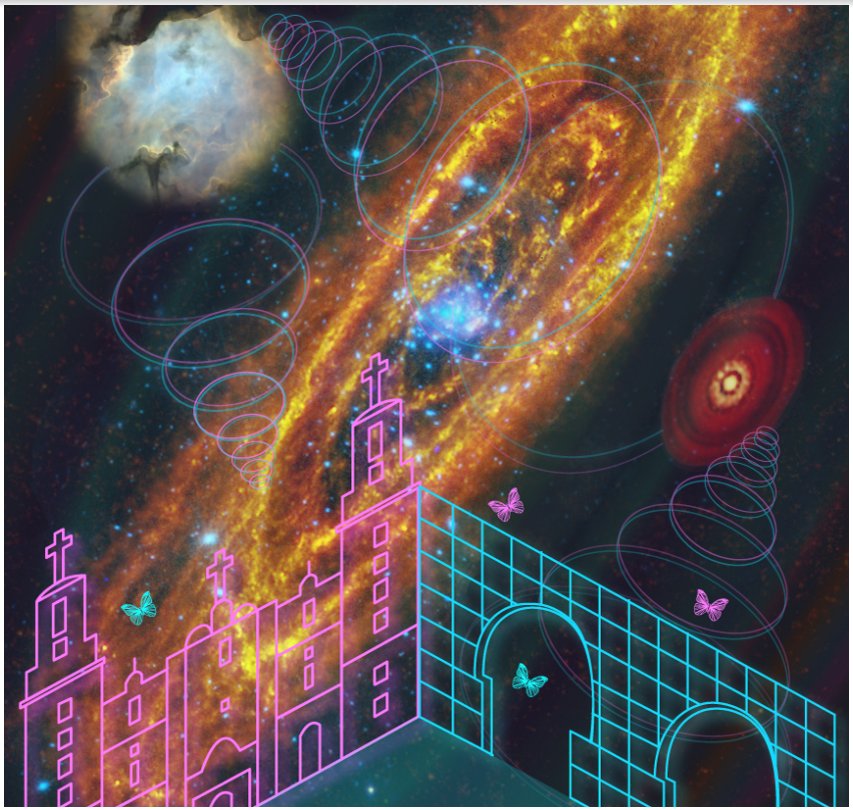

PROTOCLUSTERS

- **Progress**: full cloud, high-dynamic range, deep mapping at $\sim$ core resolution, both in continuum and lines, which has enabled to connect scales and to get a handle on the protostellar and young stellar population.
- **Unsolved questions**: to meaningfully relate these new large amounts of data to theoretical/model predictions, and to extract the important physics. E.g., what is the role of feedback at all scales/stages?

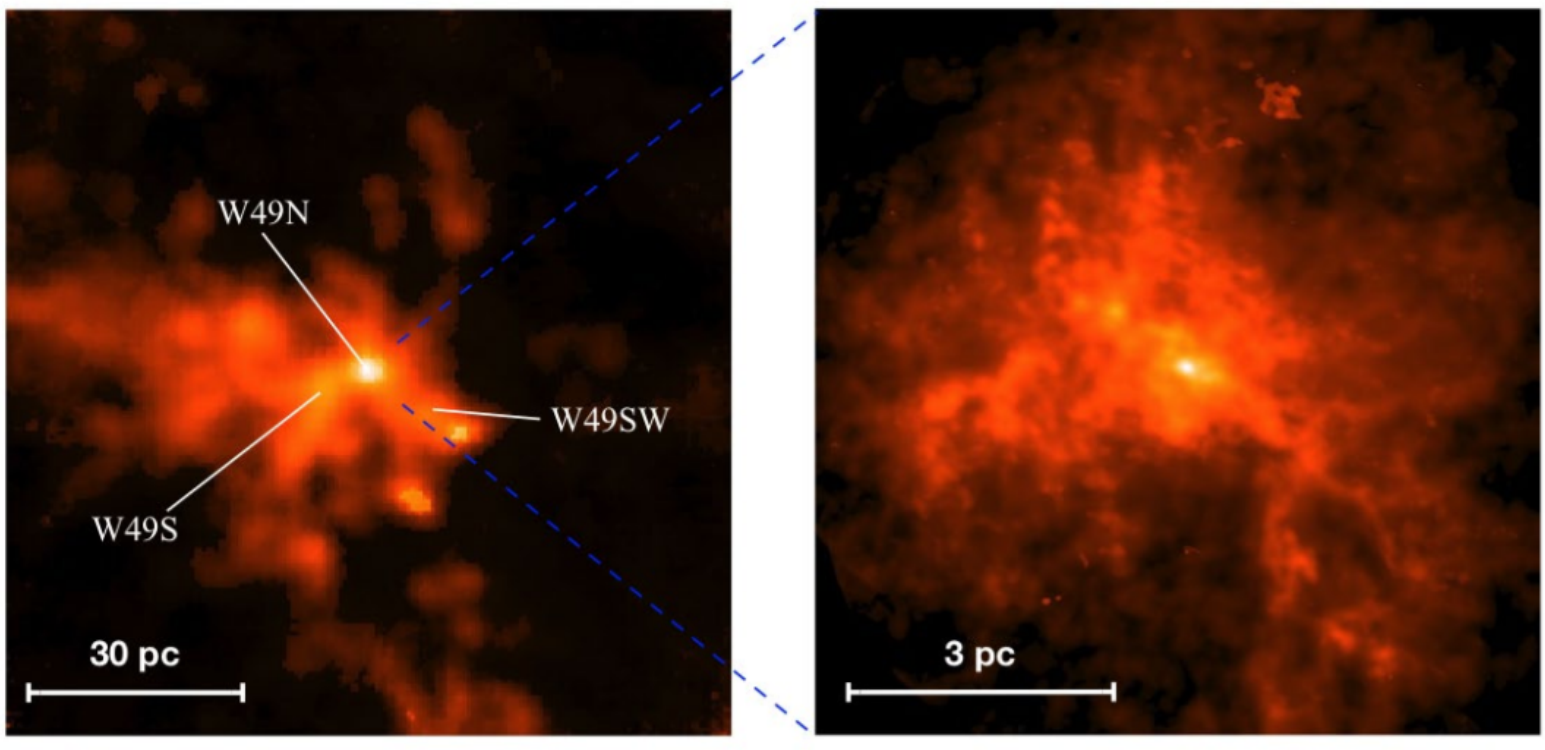

Fig: Multi-scale column density mapping of W49A (G-M et al. 2013, G-M & Liu 2014).

CORES

- **Progress**: the ability to count them across the entire range of masses, and the ability to resolve the structure of a few of them. Some seem to fragment even at < 1000 au scales.
- **Unsolved questions**: What are the population properties of these cores (e.g., CMF, see talks by Nony, Cheng). Do they tend to fragment? What is the nature of the mass flows from the outside to the inside and viceversa? Can objects be classified in an evolutionary sequence like low-mass YSOs?

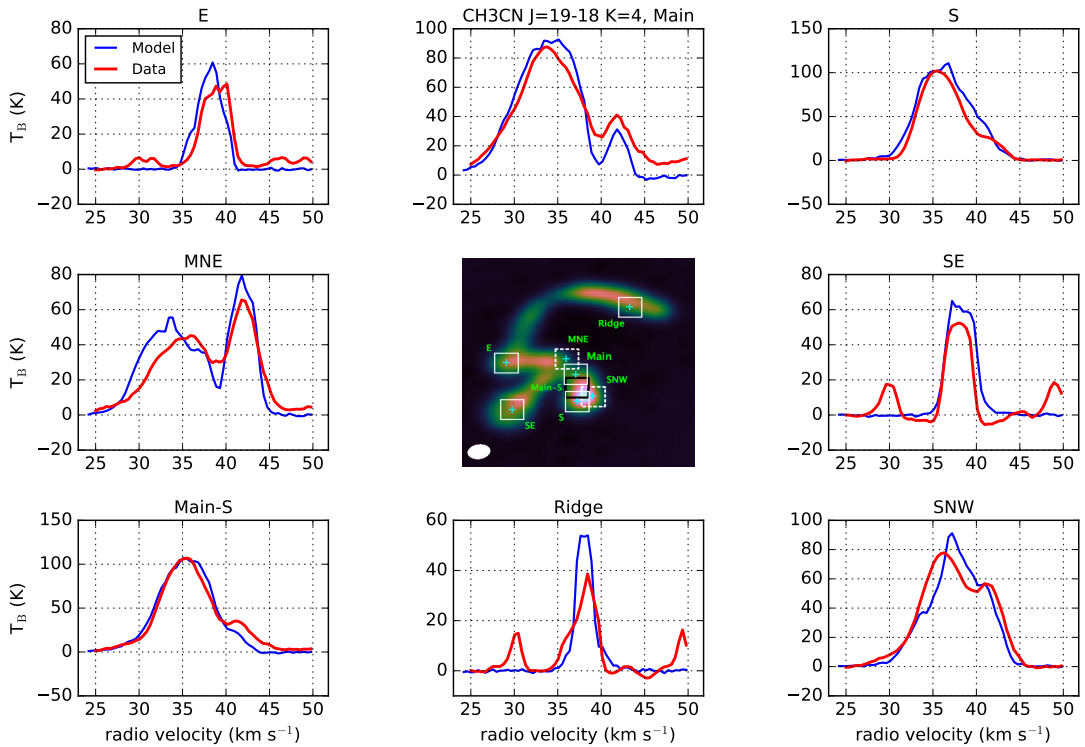

Fig: ALMA observations and model of the fragmented core W33A MM1.
Izquierdo, G-M, Maud et al. 2018.

Outline

1) Evidence for the continuity of gas flows between adjacent scales.

2) Diversity in massive cluster forming clouds and a possible origin for it.

3) On the relation of the forming stellar populations to their parent clumps and clouds.

Evidence for the continuity of gas flows between adjacent scales.

Cloud $\leftrightarrow$ Clump: converging filaments in W49A

- In W49A ($L_{\rm bol} \approx 3 \times 10^7\ L_\odot$) some filaments on ~ 10 pc scales converge in PV space toward the central clump.
- But features will only move < 1 pc over the 10^5 massive star formation timescale.

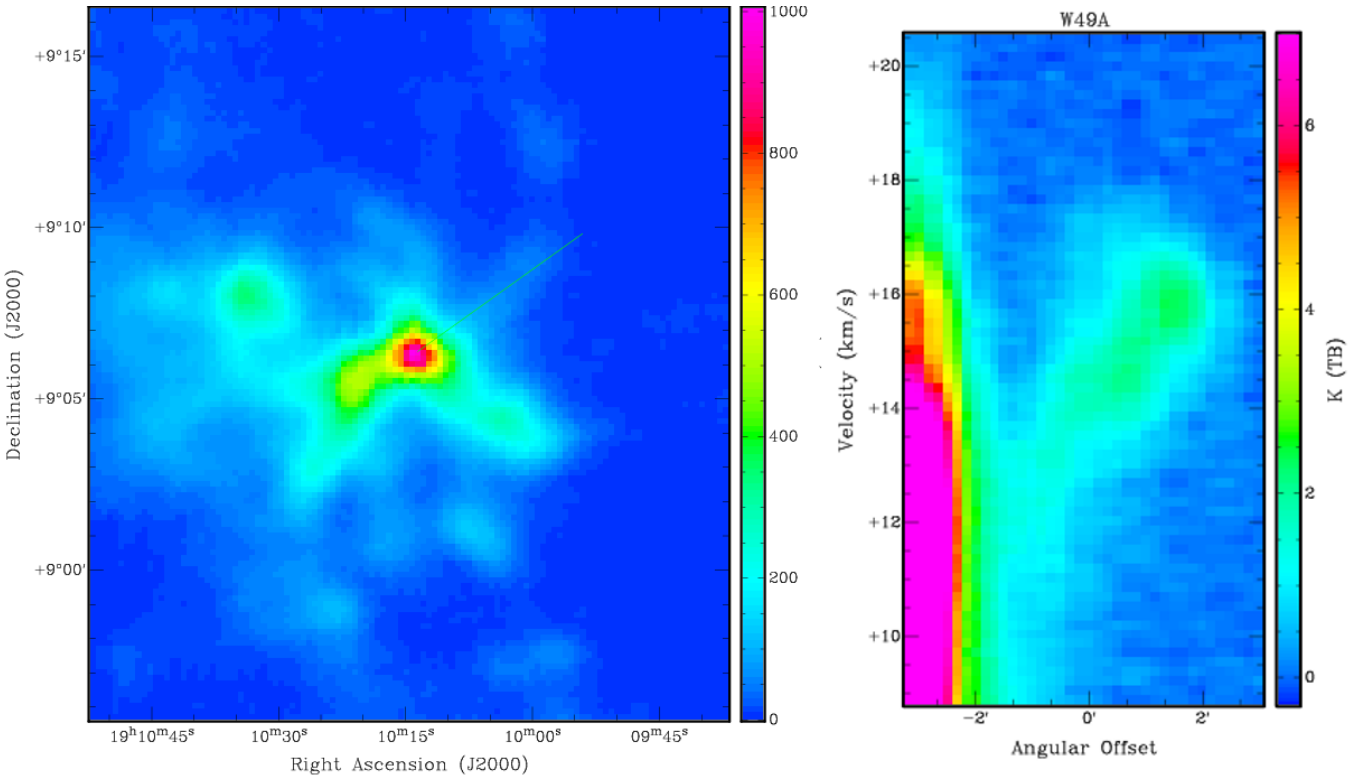

^{13}CO 1–0 PMO data from G-M, H. B. Liu, Zhi-Yu Zhang et al. 2013 (unpublished analysis).

Left: Cut in position, *Right:* Position-Velocity plot.

Clumps $\leftrightarrow$ Cores

Evidence for coherent rotation/infall from clump (1 pc) to core (0.1 pc) scales in the luminous ($L_{\rm bol} \approx 7 \times 10^5\ L_\odot$) star formation region G20.08.

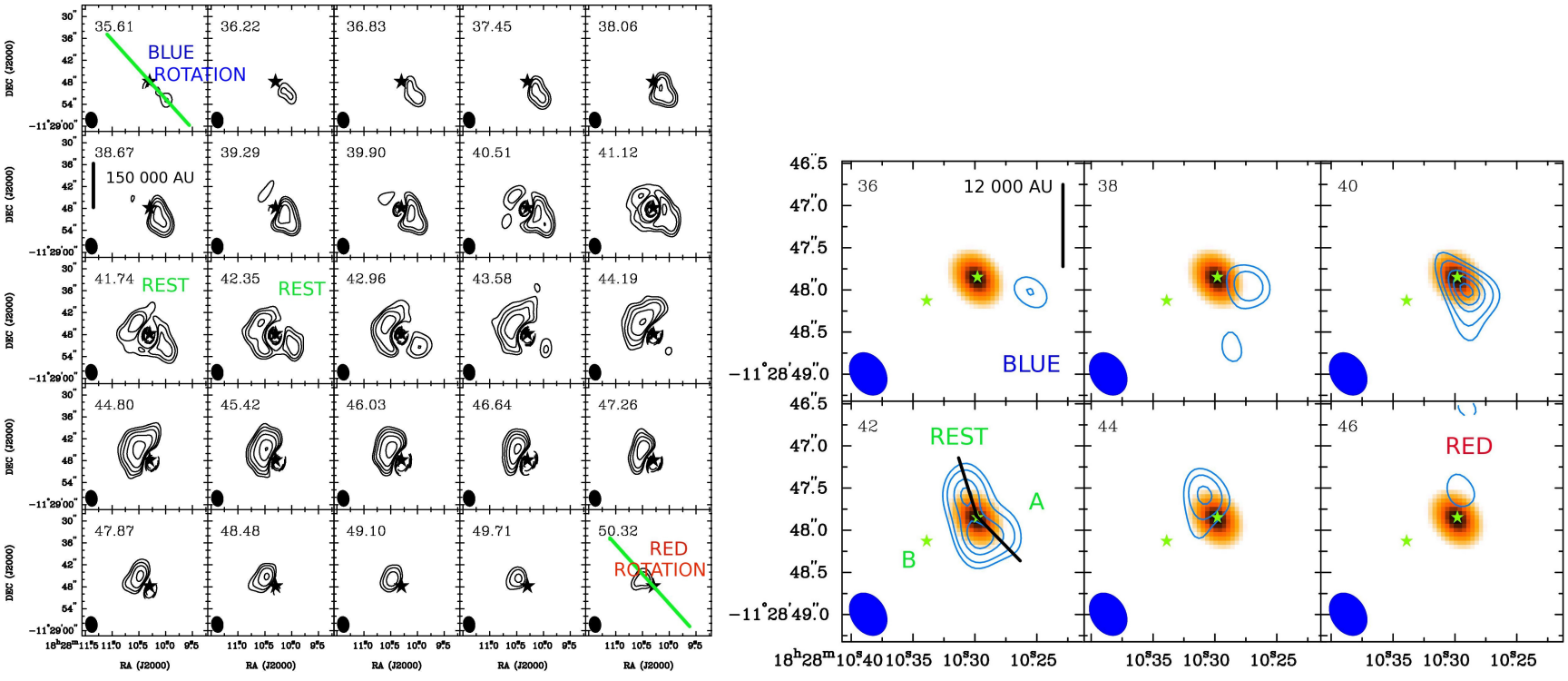

Fig: Rotation seen in NH_3 emission with VLA-D on parsec scales and CH_3CN with SMA-VEX on 0.1 pc scales. G-M, Keto, Zhang+2009.

Clumps $\leftrightarrow$ Cores

- Evidence for coherent rotation/infall from clump (1 pc) to core (0.1 pc) scales in the luminous ($L_{\rm bol} \approx 7 \times 10^5\ L_\odot$) star formation region G20.08.
- Also P. Barnes+2010, Y. Contreras poster.

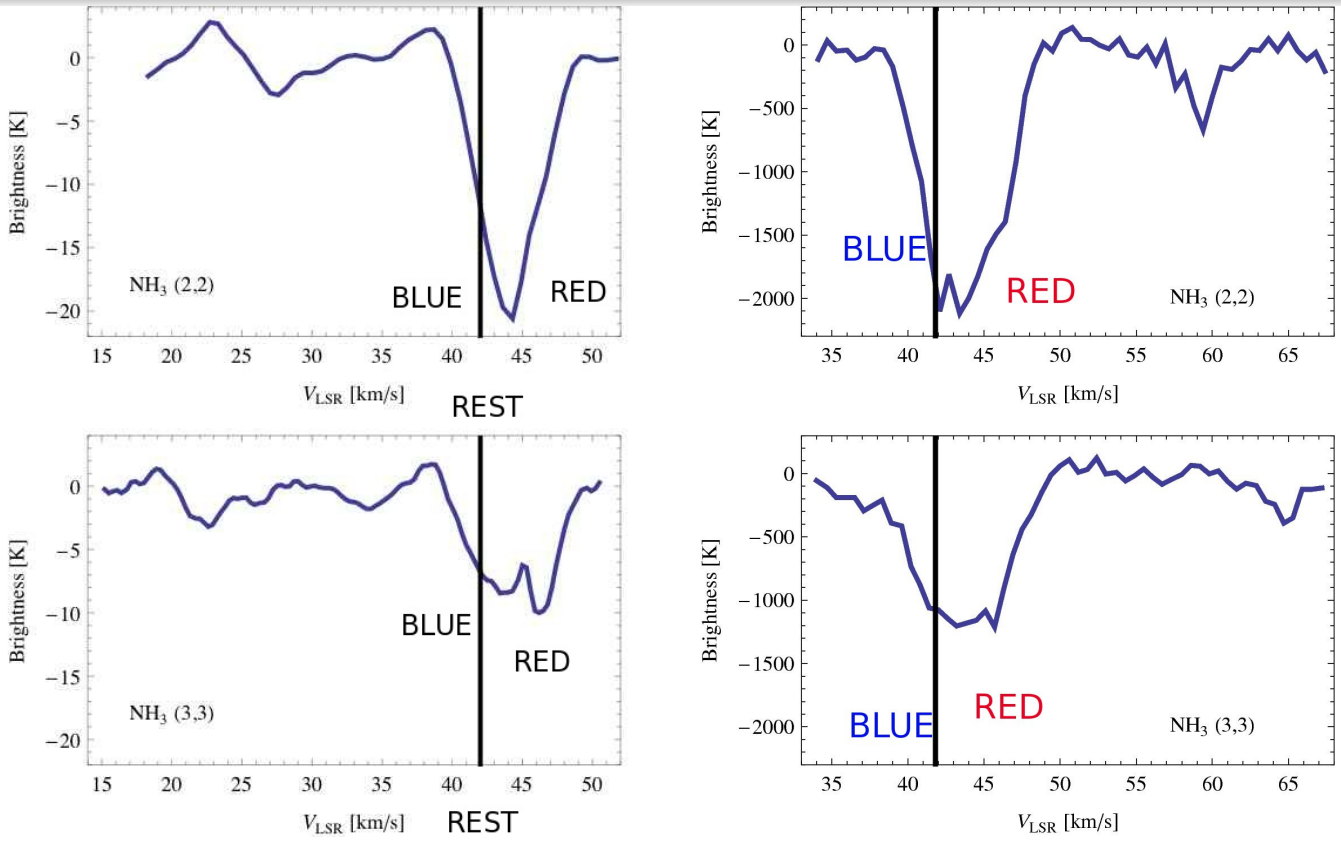

Fig: Infall seen in NH_3 absorption against the backlight UCHIIs with VLA-D in clump scales and with VLA-B in core scales. G-M, Keto, Zhang+2009.

Clumps (filaments)↔ Cores

- Massive star formation at the center of converging, pc-scale filaments in W33A ($L_{\rm bol} \approx 4 \times 10^4\ L_\odot$).
- Other examples: Schneider+2010, Peretto+2013, Juárez+, Treviño-Morales+, Posters by Contreras, V. Chen. Walker Lu.

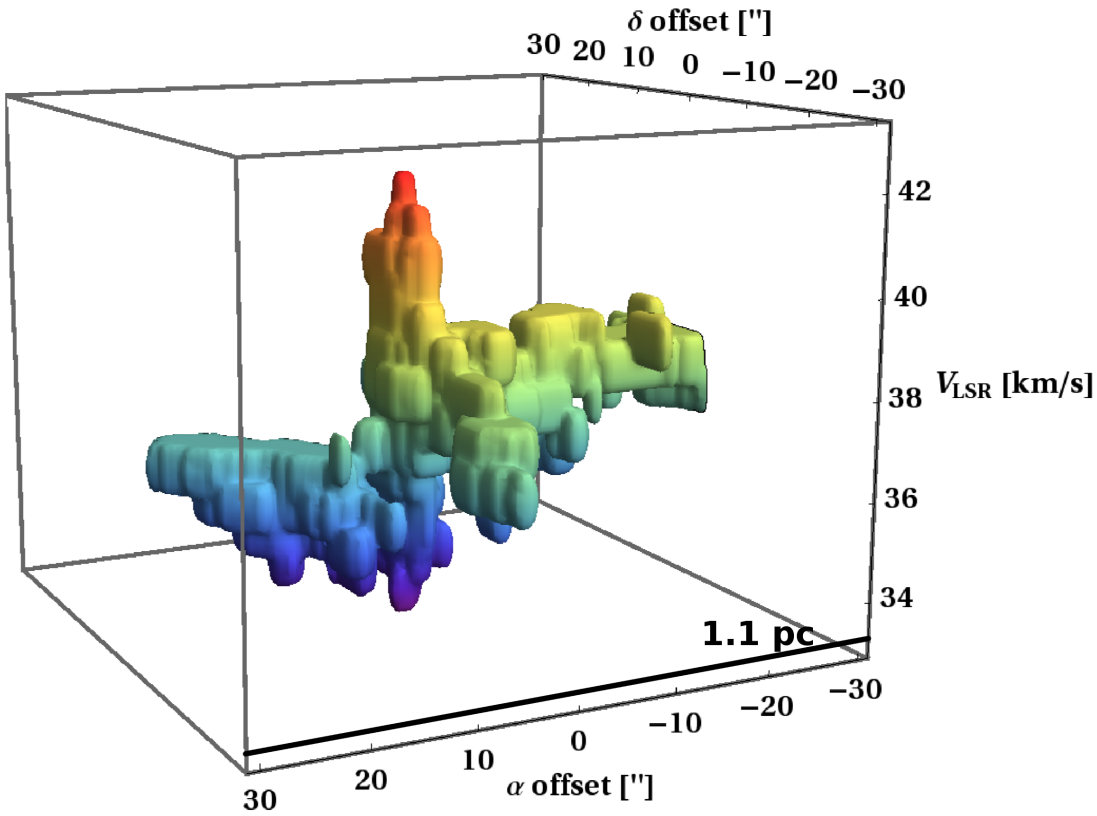

Fig: PPV rendering of filaments seen in NH_3 with VLA-D. G-M, Zhang, Keto+2010.

Clumps (filaments)$\leftrightarrow$ Cores

- Massive star formation at the center of converging, pc-scale filaments in W33A ($L_{\rm bol} \approx 4 \times 10^4\ L_\odot$).
- Other examples: Schneider+2010, Juárez+17, Treviño-Morales+.

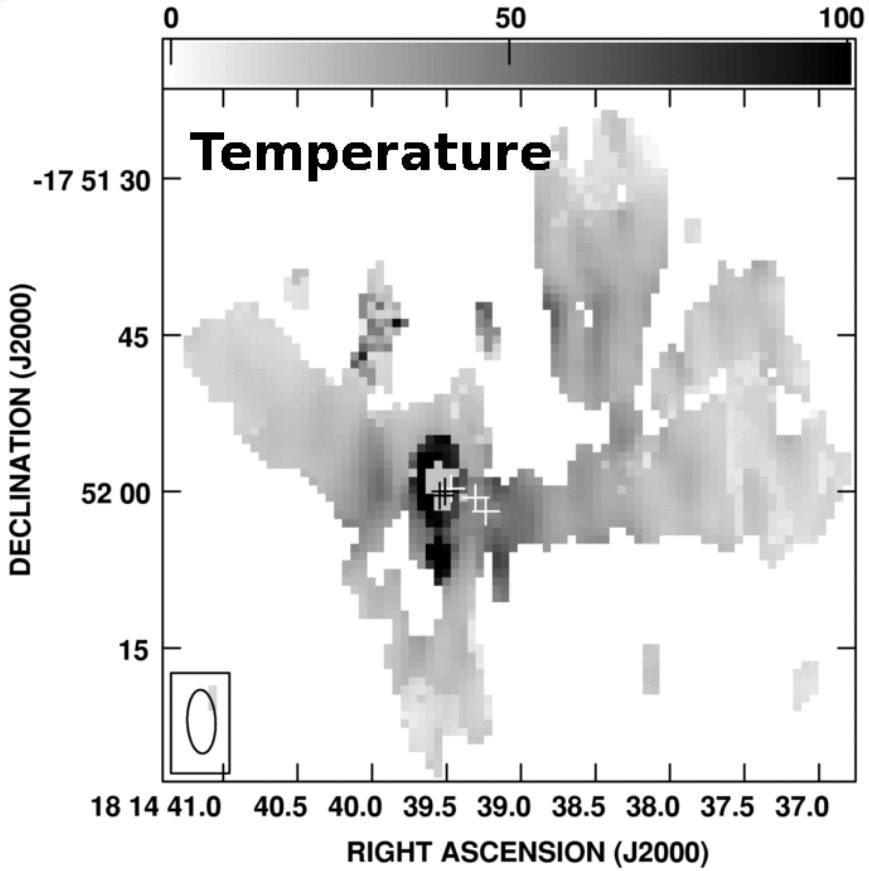

Fig: Heating due to massive star formation at the intersection of filaments.

G-M, Zhang, Keto+2010.

Cores $\leftrightarrow$ Disks

W33A: massive ($M \sim 15\ M_{\odot}$) YSO with a disk?, or a multiple system of forming massive/intermediate mass stars?

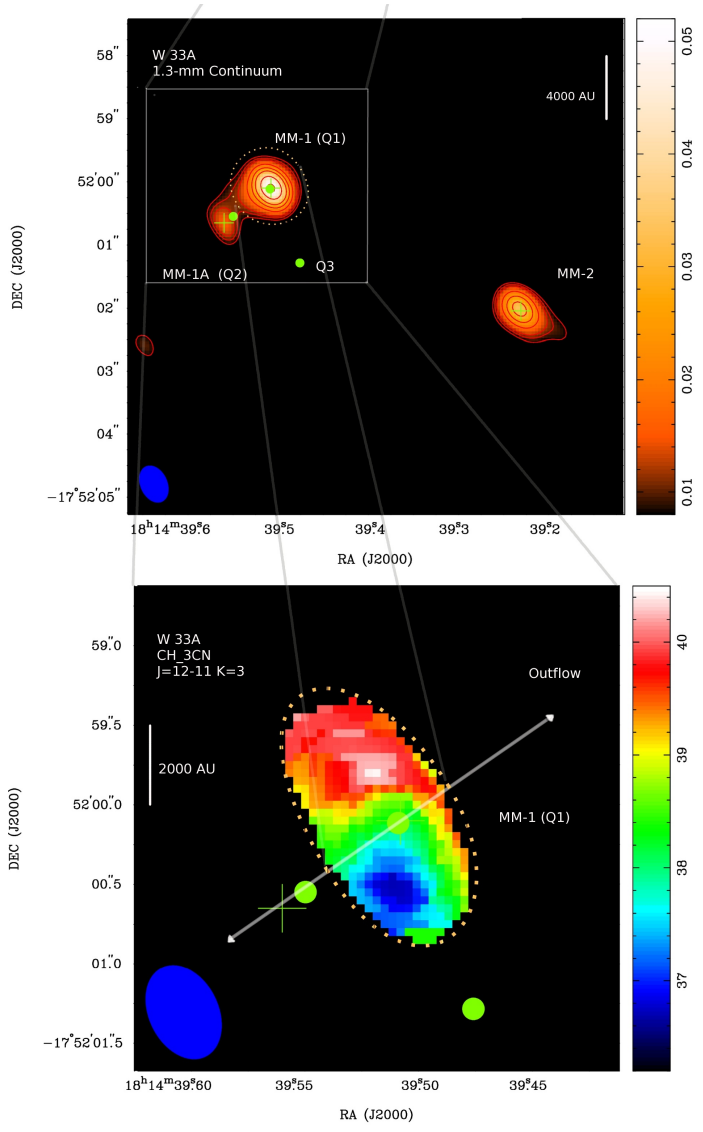

Fig: previous (SMA) view of the heart of W33A.

Cores $\leftrightarrow$ Disks

Spiral-like filament feeding a multiple system of massive stars.
See Luke Maud's talk today.
New radiative transfer model (using LIME) developed by student Andrés Izquierdo (Izquierdo, G-M, Maud et al. 2018).

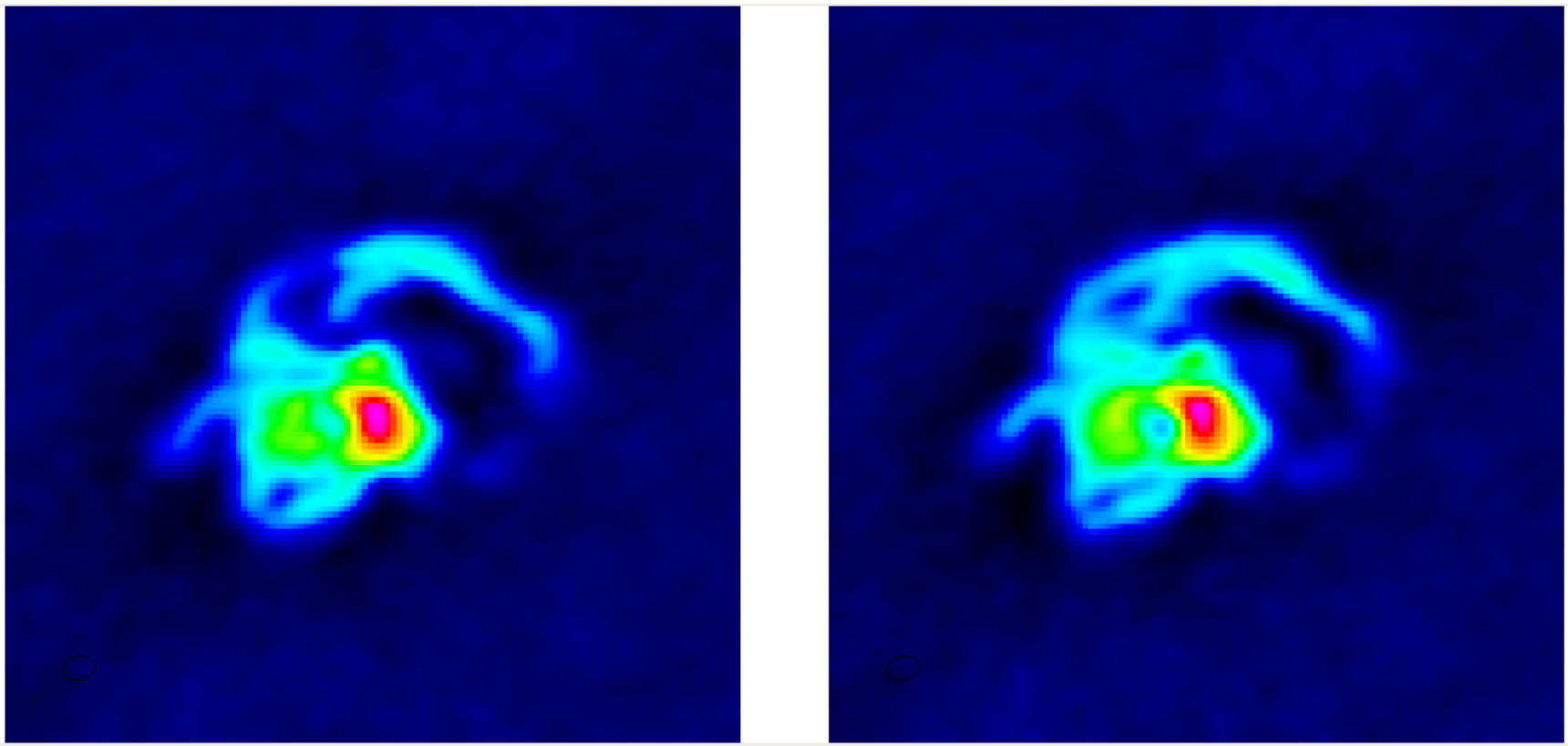

Fig: reality with ALMA observations of CH_3CN at 0.17" = 400 au resolution.

Maud, Hoare, G-M et al. 2017.

Results: K = 4 spectra of compact sources

- All synthetic images from LIME are passed through the ALMA response in CASA.

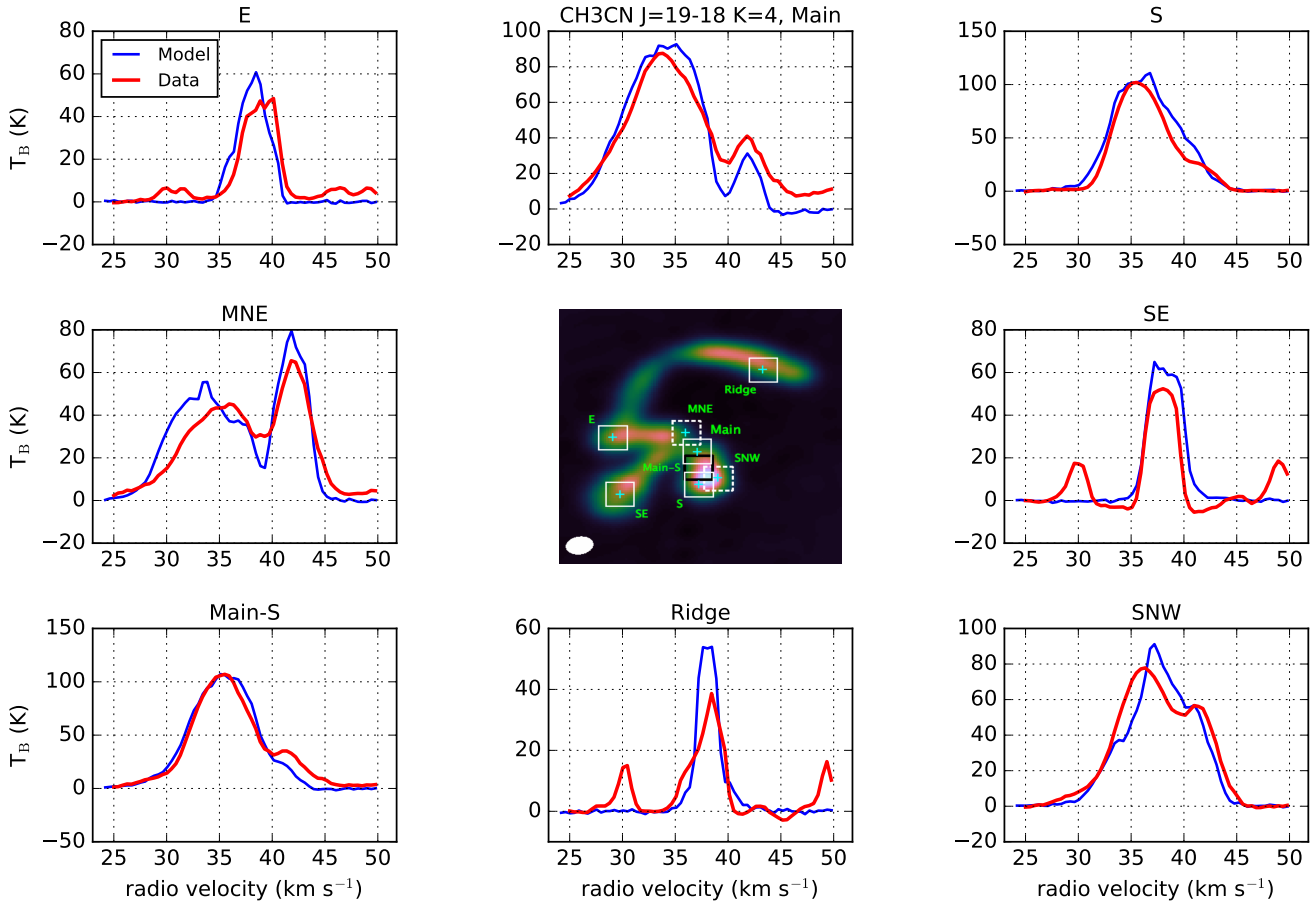

Fig: comparison of real and simulated CH_3CN $J = 19 - 18$, $K = 4$ ($E_U = 282$ K) spectra as observed with ALMA at 0.17 arcsec (400 au) resolution.

Results: comparison of extended spectra

- OK, but some extended emission is missing.

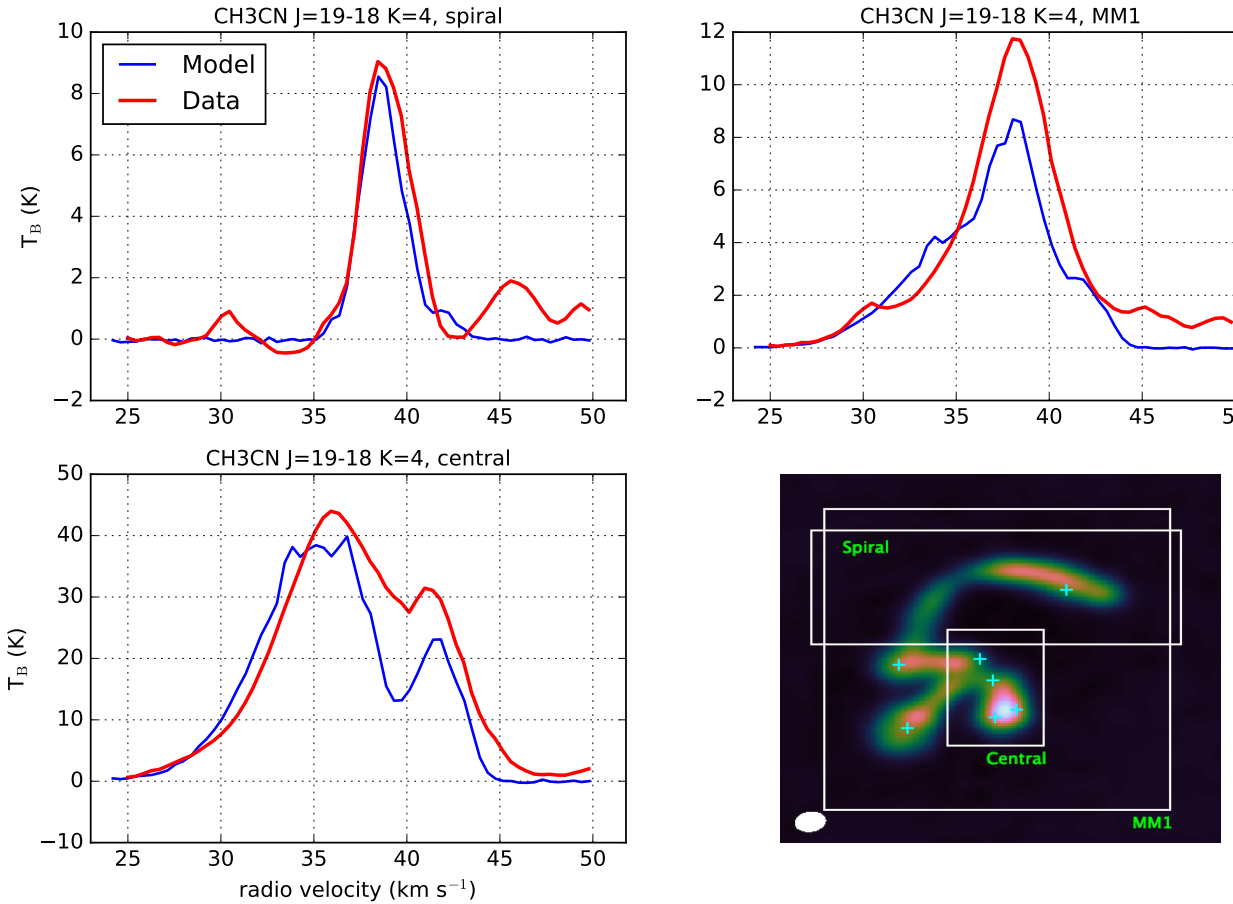

Fig: comparison of real and simulated CH_3CN $J = 19 - 18$, $K = 4$ ($E_U = 282$ K) spectra over selected extended regions.

Results: comparison of moment maps

- Integrated intensity, (complex) velocity field, and dispersion are well reproduced.
- Some extended emission is missing.

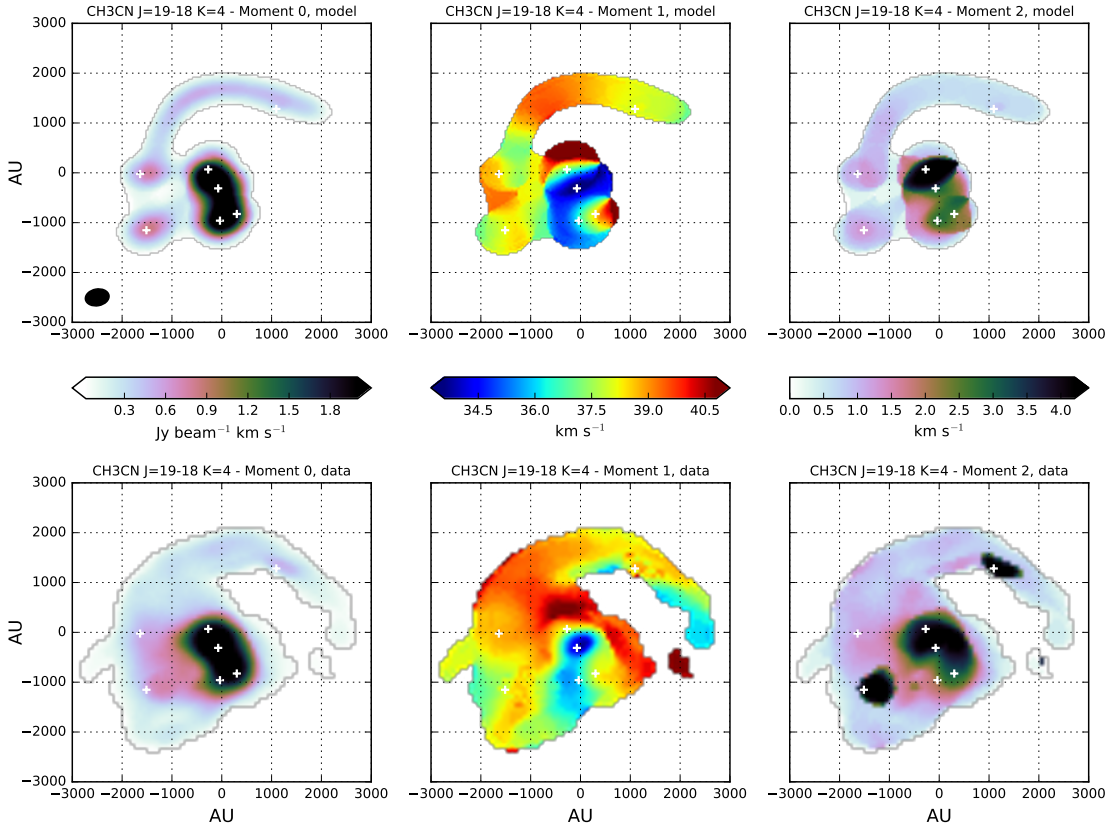

Fig: comparison of real and simulated CH_3CN $J = 19 - 18$, $K = 4$ ($E_U = 282$ K) moment maps as observed with ALMA at 0.17 arcsec (400 au) resolution.

Diversity in massive cluster forming clouds and a possible origin for it.

CLOUD STRUCTURE OF LUMINOUS CLUSTER-FORMING CLOUDS

- Master thesis of Yuxin Lin (now in Bonn) with Baobab Liu and Di Li.
- Column density, temperature, and luminosity maps of several of the 'monster' MW clouds at 10" ($\sim$ 0.2 pc) resolution using their Herschel/Planck + CSO/JCMT Fourier combination technique.

Source Information

Target Source	R.A. (J2000)	decl. (J2000)	Distance (kpc)	Mass[a] ($M_\odot$)	Luminosity[a] ($L_\odot$)	Reference[b]
W49A	$19^h10^m13\overset{s}{.}000$	$09°06'00\overset{''}{.}00$	$11.4^{+1.2}_{-1.2}$	2.30×10^5	3.67×10^7	Zhang et al. (2013)
W43-main	$18^h47^m36\overset{s}{.}427$	$-01°59'02\overset{''}{.}48$	$5.49^{+0.39}_{-0.34}$	1.32×10^5	1.23×10^7	Zhang et al. (2014)
W43-south	$18^h46^m02\overset{s}{.}084$	$-02°43'00\overset{''}{.}83$	$5.49^{+0.39}_{-0.34}$	6.43×10^4	6.29×10^6	Zhang et al. (2014)
G10.2-0.3	$18^h09^m23\overset{s}{.}000$	$-20°16'17\overset{''}{.}00$	$4.95^{+0.51}_{-0.43}$	1.03×10^5	6.43×10^6	Corbel & Eikenberry (2004)[c]
G10.6-0.4	$18^h10^m29\overset{s}{.}26$	$-19°55'59\overset{''}{.}5$	$4.95^{+0.51}_{-0.43}$	2.33×10^4	3.20×10^6	Sanna et al. (2014)
W33	$18^h14^m13\overset{s}{.}65$	$-17°55'38\overset{''}{.}9$	$2.40^{+0.17}_{-0.15}$	3.63×10^4	2.43×10^6	Immer et al. (2013)
G10.3-0.1	$18^h08^m58\overset{s}{.}000$	$-20°05'15\overset{''}{.}00$	$3.22^{+0.12}_{-0.12}/2.56^{+0.28}_{-0.28}$	$2.70 \times 10^4/1.70 \times 10^4$	$1.54 \times 10^6/9.71 \times 10^5$	Kazi Rygl, Katharina Immer[d]

Fig: source sample of Lin, Liu, Li et al. 2016.

A VARIETY OF CLUSTER-FORMING CLOUDS

Variety in massive cluster forming clouds:
- Concentrated vs more extended morphologies.
- Prominent high-N tails vs relative lack of high-N gas.

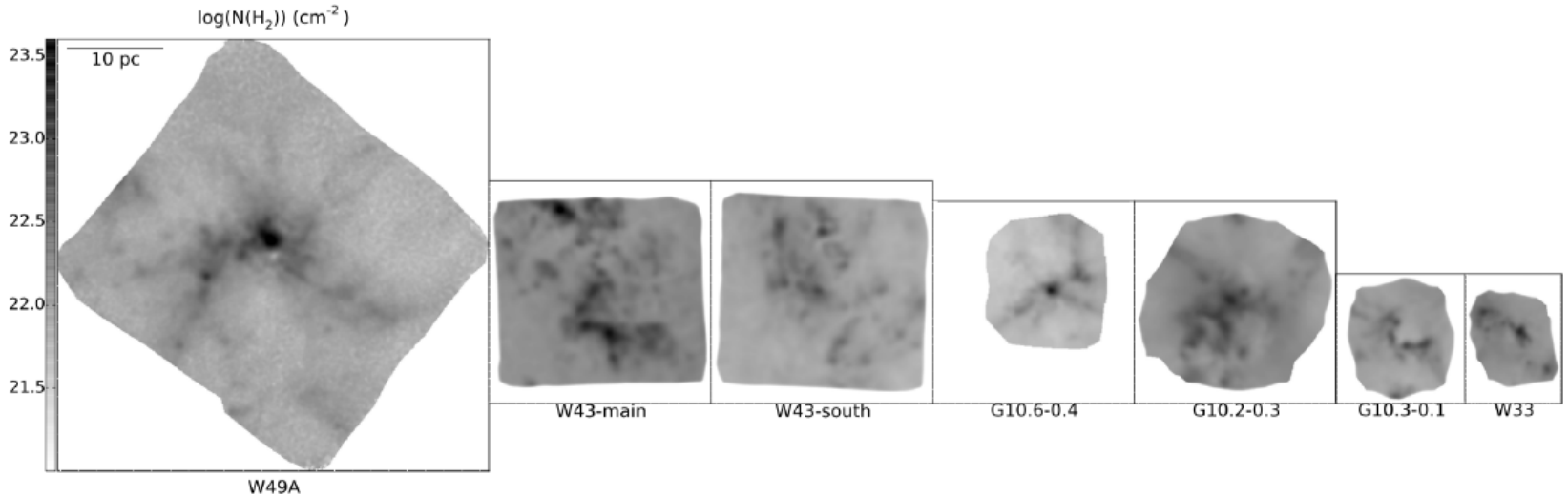

Fig: Column maps from first sample set to absolute scale (Lin, Liu, Li+2016).

A VARIETY OF CLUSTER-FORMING CLOUDS

Variety in massive cluster forming clouds:
- Concentrated vs more extended morphologies.
- Prominent high-N tails vs relative lack of high-N gas.

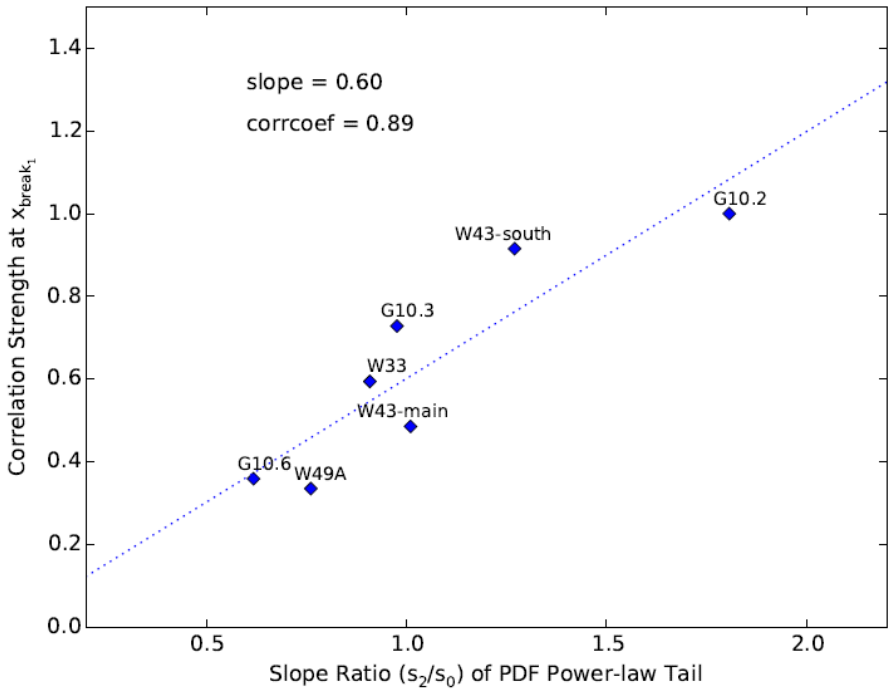

Fig: The more concentrated cloud morphology is, the more prominent (less steep) the high-N power law tail (Lin, Liu, Li+2016).

ON THE ORIGIN OF THE MORPHOLOGICAL DIFFERENCES

- Hypothesis: mainly due to the initial level of angular momentum (shear/rotation), with some influence of turbulence and B-field.

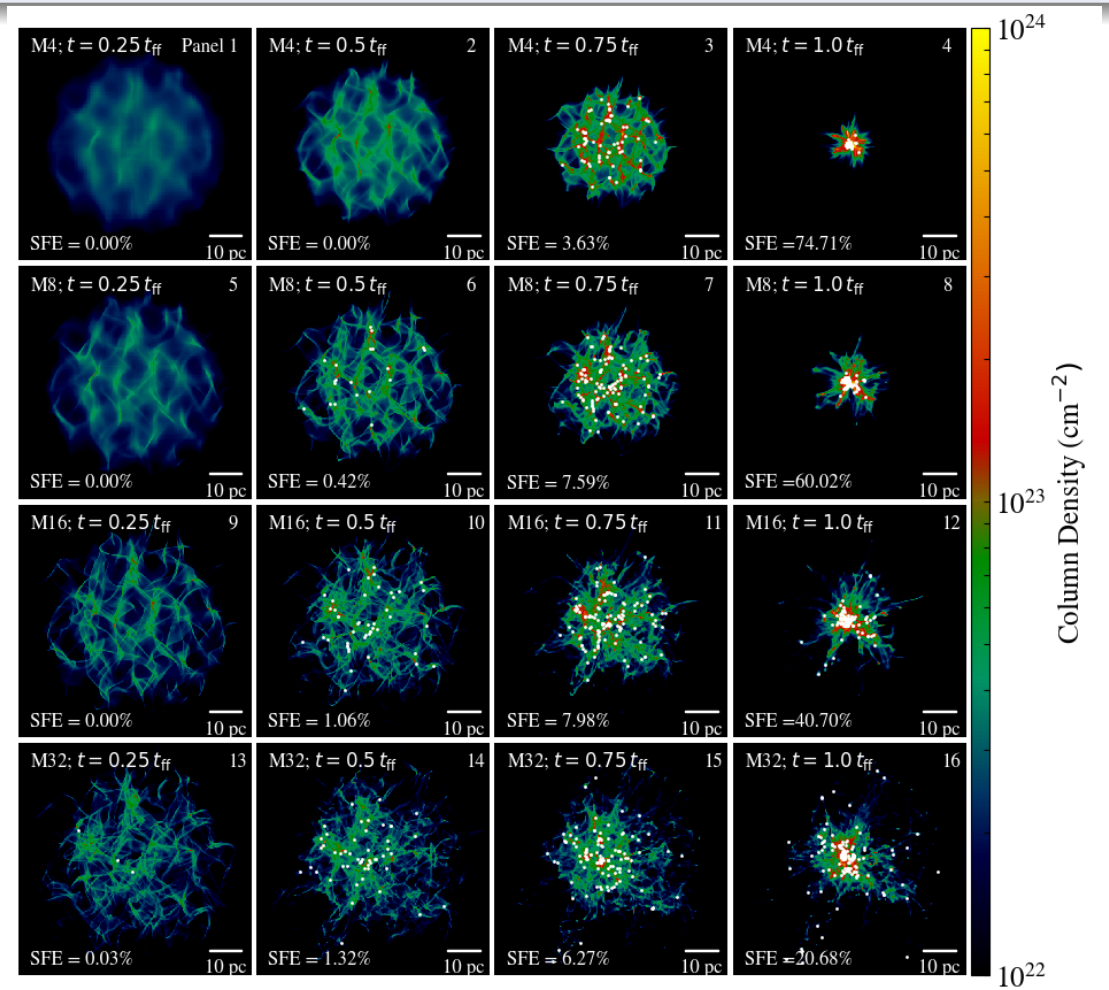

Fig: Simulations of a massive (10^6 $M_\odot$) cluster forming cloud with initial turbulence but NO shear/rotation.
Zamora-Avilés, G-M, Ballesteros-Paredes+, in prep.

ON THE ORIGIN OF THE MORPHOLOGICAL DIFFERENCES

- Hypothesis: mainly due to the initial level of angular momentum (shear/rotation), with some influence of turbulence and B-field.

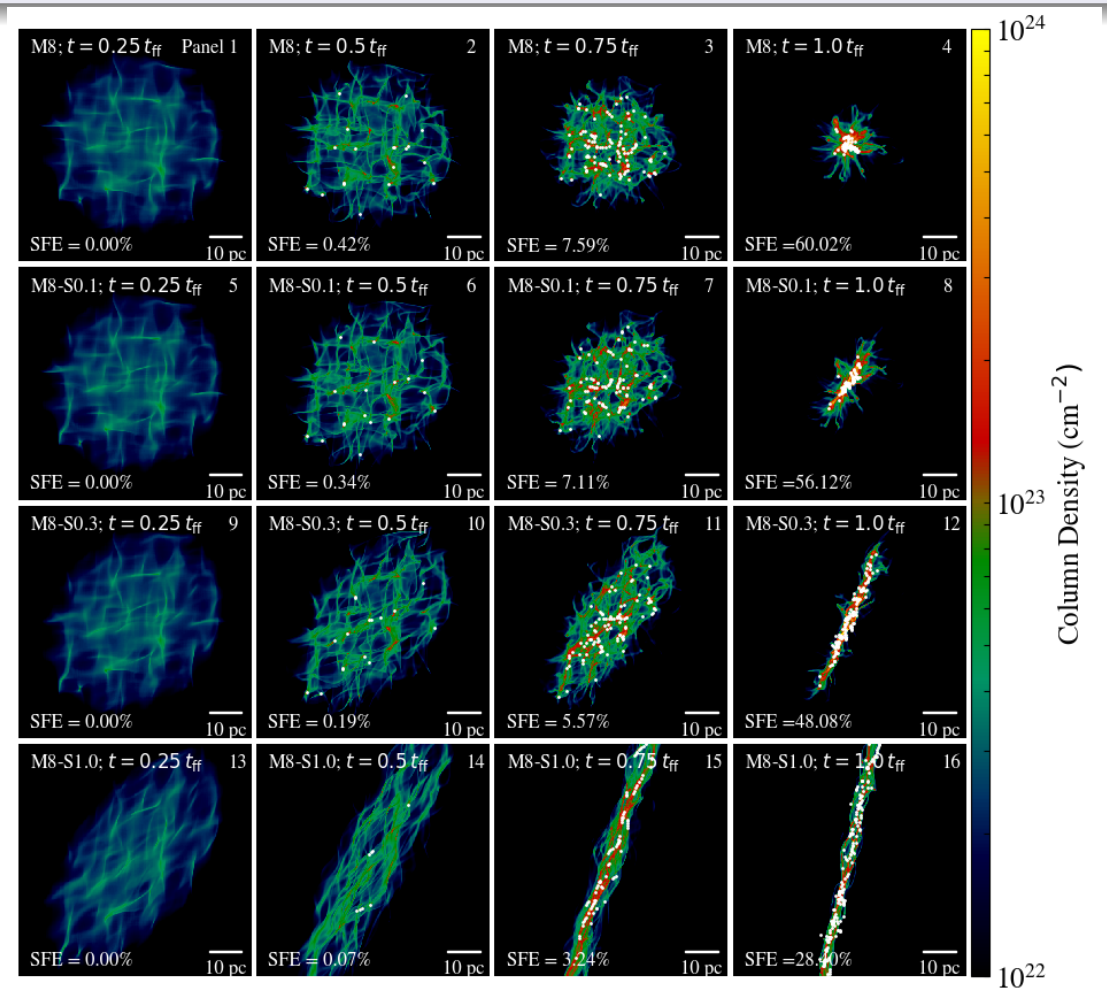

Fig: Simulations of a massive (10^6 $M_\odot$) cluster forming cloud with initial turbulence AND shear. Zamora-Avilés, G-M, Ballesteros-Paredes+, in prep.

ON THE ORIGIN OF THE MORPHOLOGICAL DIFFERENCES

- Hypothesis: mainly due to the initial level of angular momentum (shear/rotation), with some influence of turbulence and B-field.

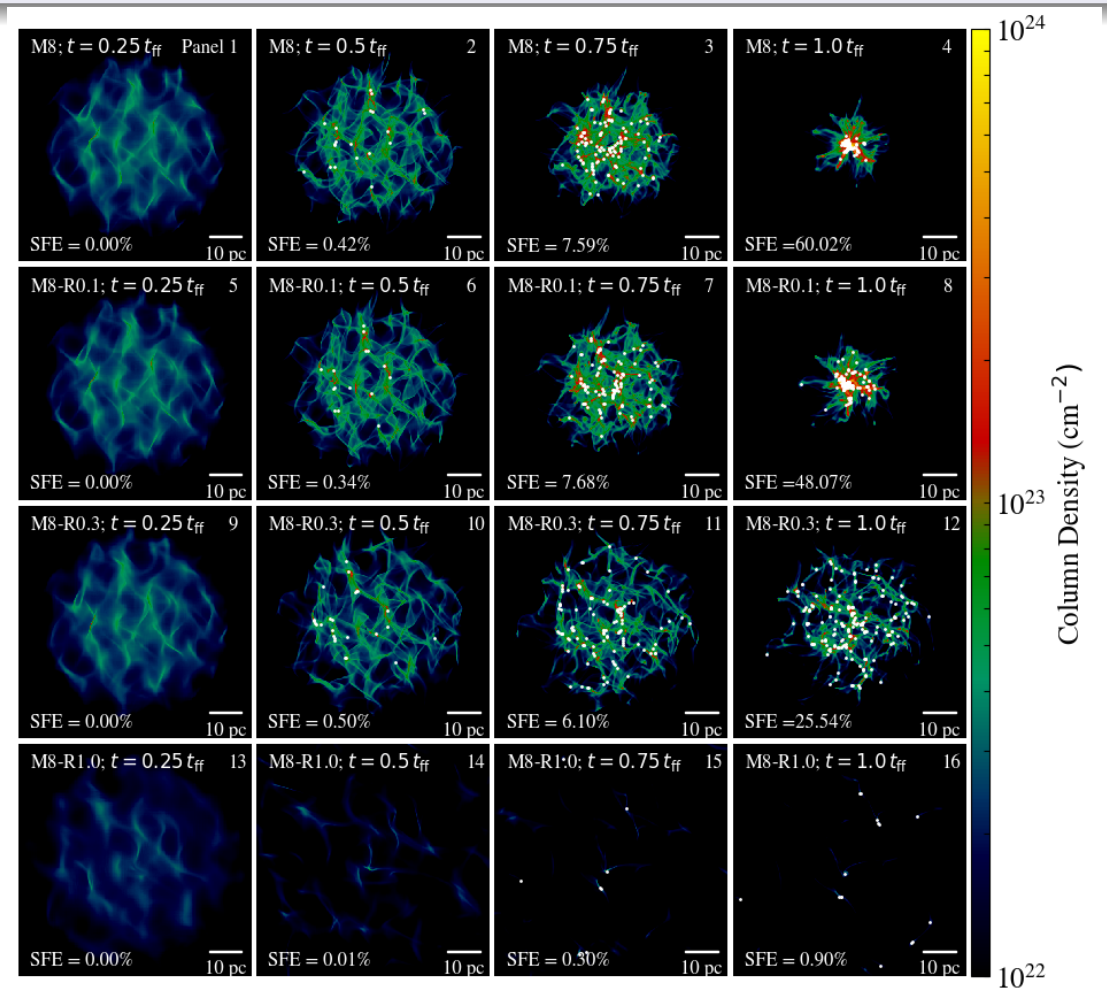

Fig: Simulations of a massive (10^6 $M_\odot$) cluster forming cloud with initial turbulence AND rotation. Zamora-Avilés, G-M, Ballesteros-Paredes+, in prep.

OBSERVATIONAL EVIDENCE FOR CLOUD ROTATION AND SHEAR?

- Shear can be important in some clouds.
- There are some reports of possible rotation.

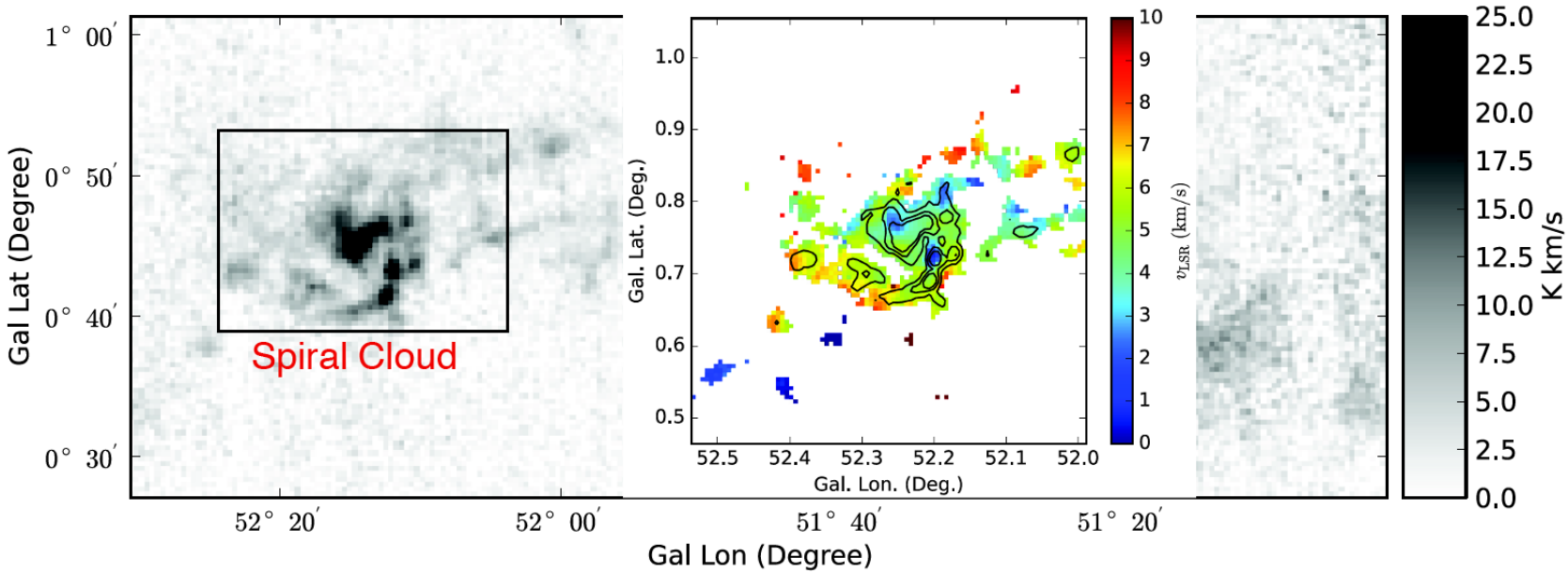

Fig: spiral cloud with possible rotation reported by Guang Xing Li et al. 2017, seen in ^{13}CO 1–0.

Fragmented Spiral Clump G33.92+0.11

Evidence for flattened accretion flows at clump scale.

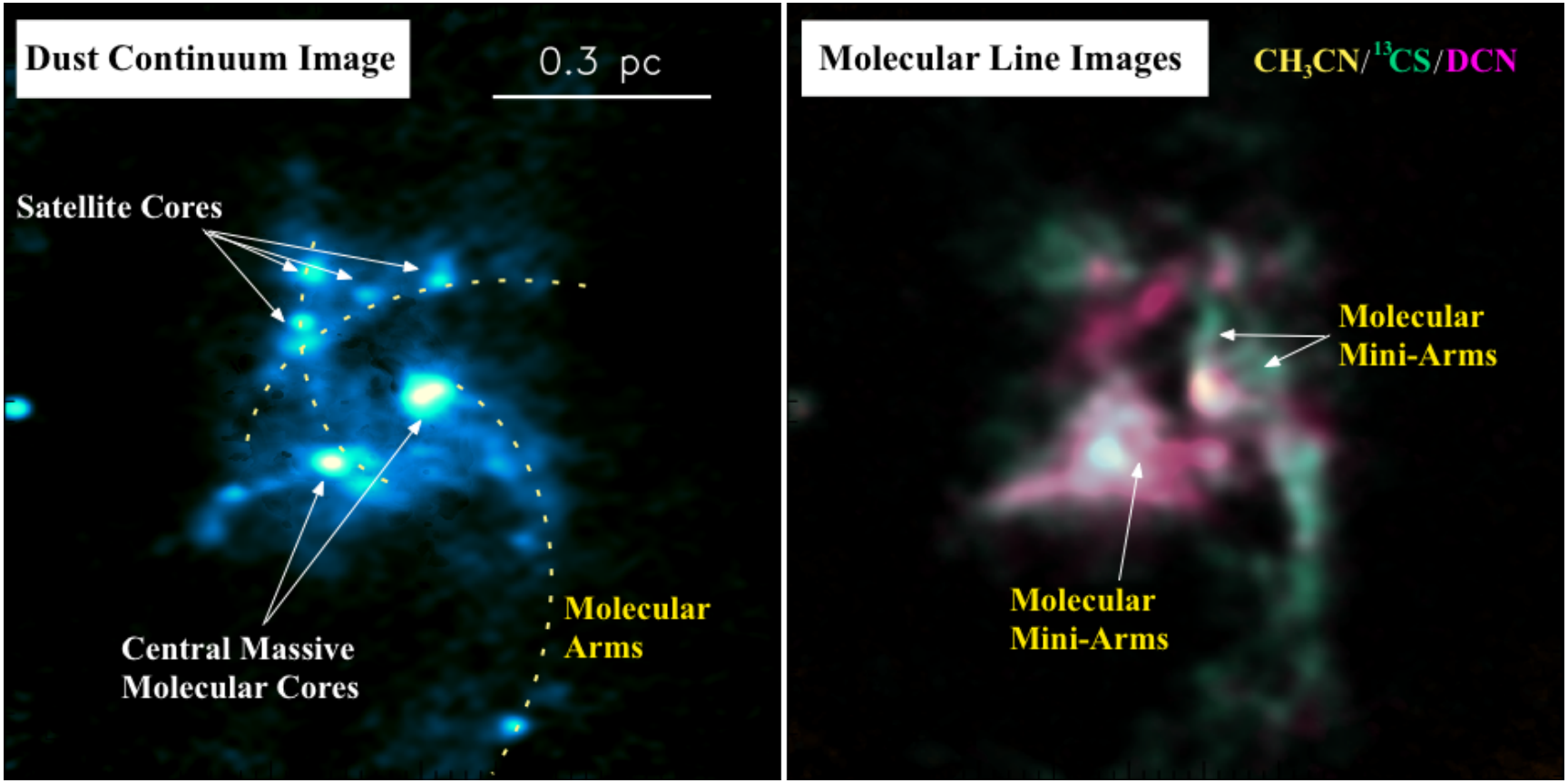

Fig: ALMA discovery of spiral structure and chemical stratification in the cluster-forming molecular clump G33.92.
Baobab Liu, G-M, Jiménez-Serra et al. (2015).

Fragmented Spiral Clump G33.92+0.11

Evidence for flattened accretion flows at clump scale.

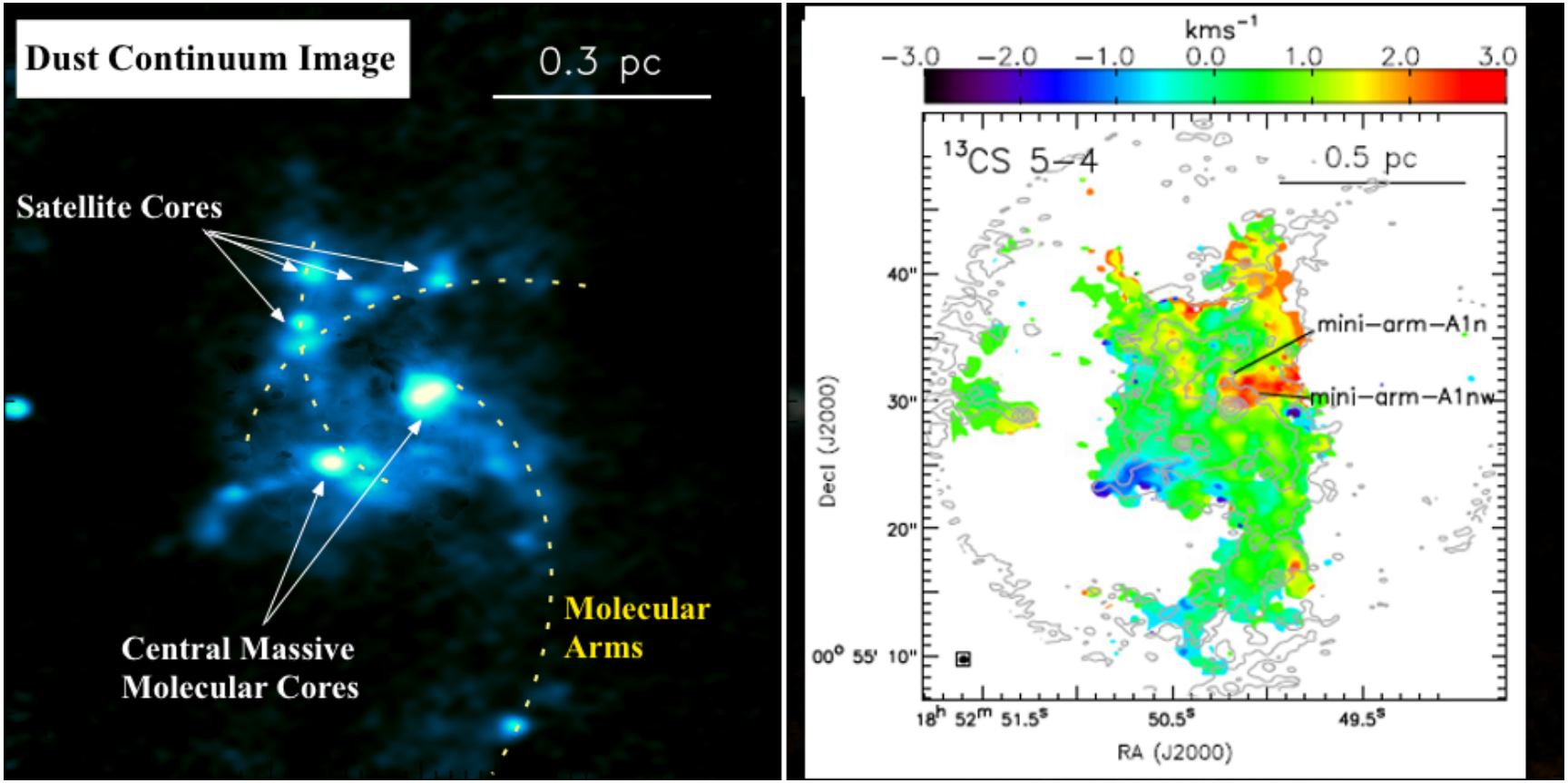

Fig: ALMA discovery of spiral structure and chemical stratification in the cluster-forming molecular clump G33.92.
Baobab Liu, G-M, Jiménez-Serra et al. (2015).

LOCATION AND ENVIRONMENT?

- Local potential molecular and neutral gas reservoir.
- Galactic kinematics.

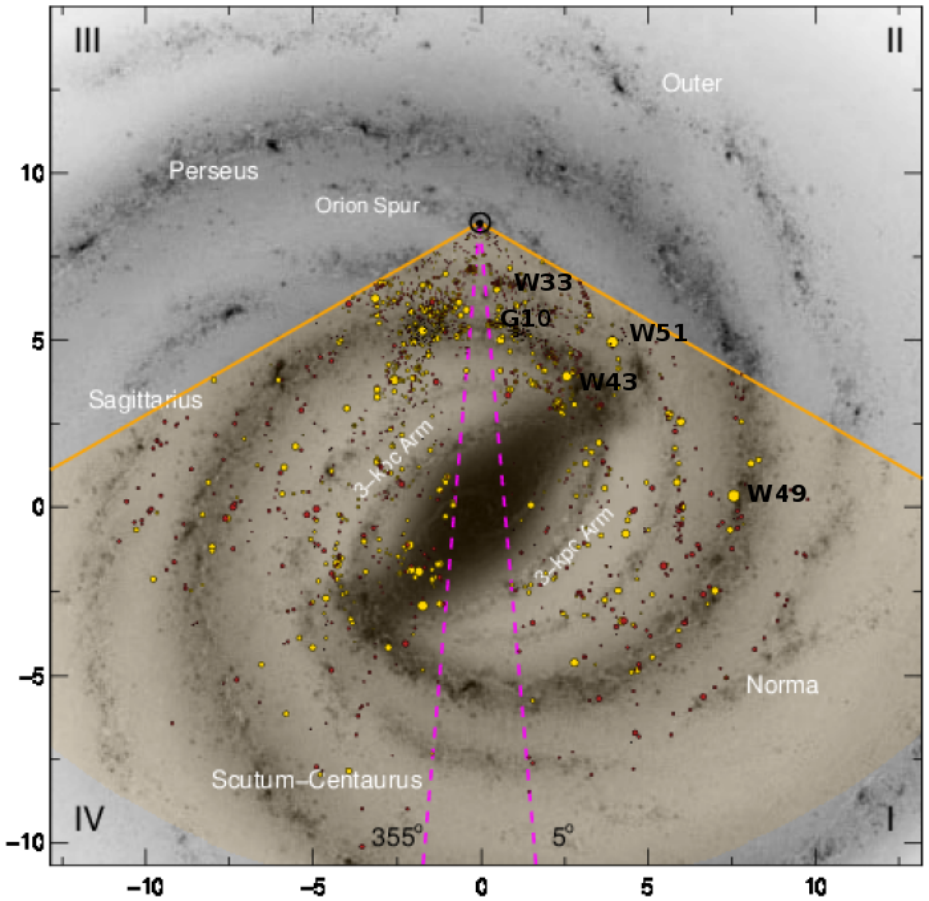

Fig: Some Galactic monsters approximated location. Modified from Urquhart+2018.

The forming stellar populations and their relation to their parent clumps and clouds.

The Forming Stellar Populations

Several overlapping components:
- Pre- and proto-stellar cores and their substructure → ALMA (talks by Motte, Nony, Cheng).
- Embedded young stellar population → ALMA, (ng)VLA (talk by Dzib), JWST (Posters by Kendrew, M. Liu).
- Not so embedded young stellar population → (ng)VLA, Chandra, OIR facilities (posters by Towner, Lumsden).

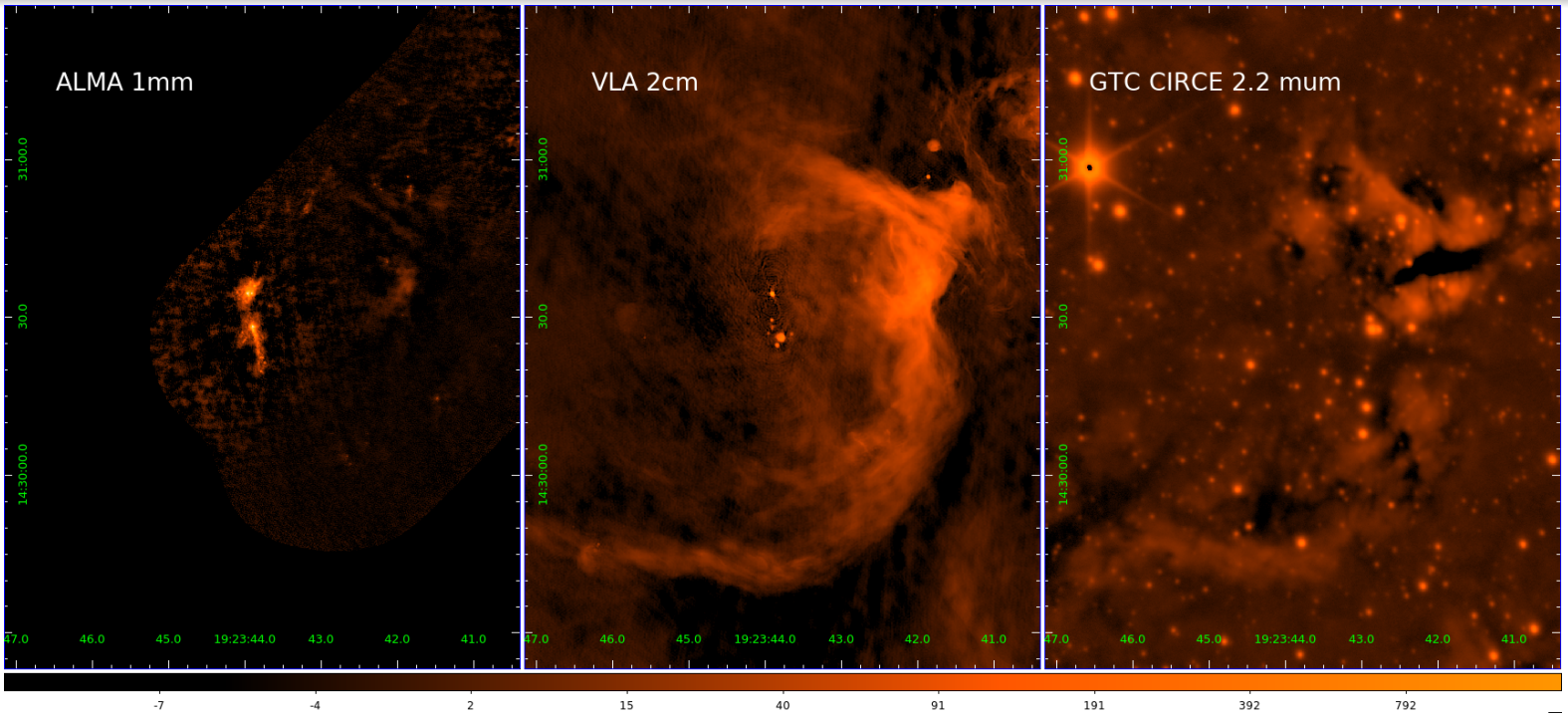

Fig: ALMA/VLA/GTC view of W51A Main. The associated compact source catalogues are almost mutually exclusive. In prep. with Román-Zúiga and and Ginsburg.

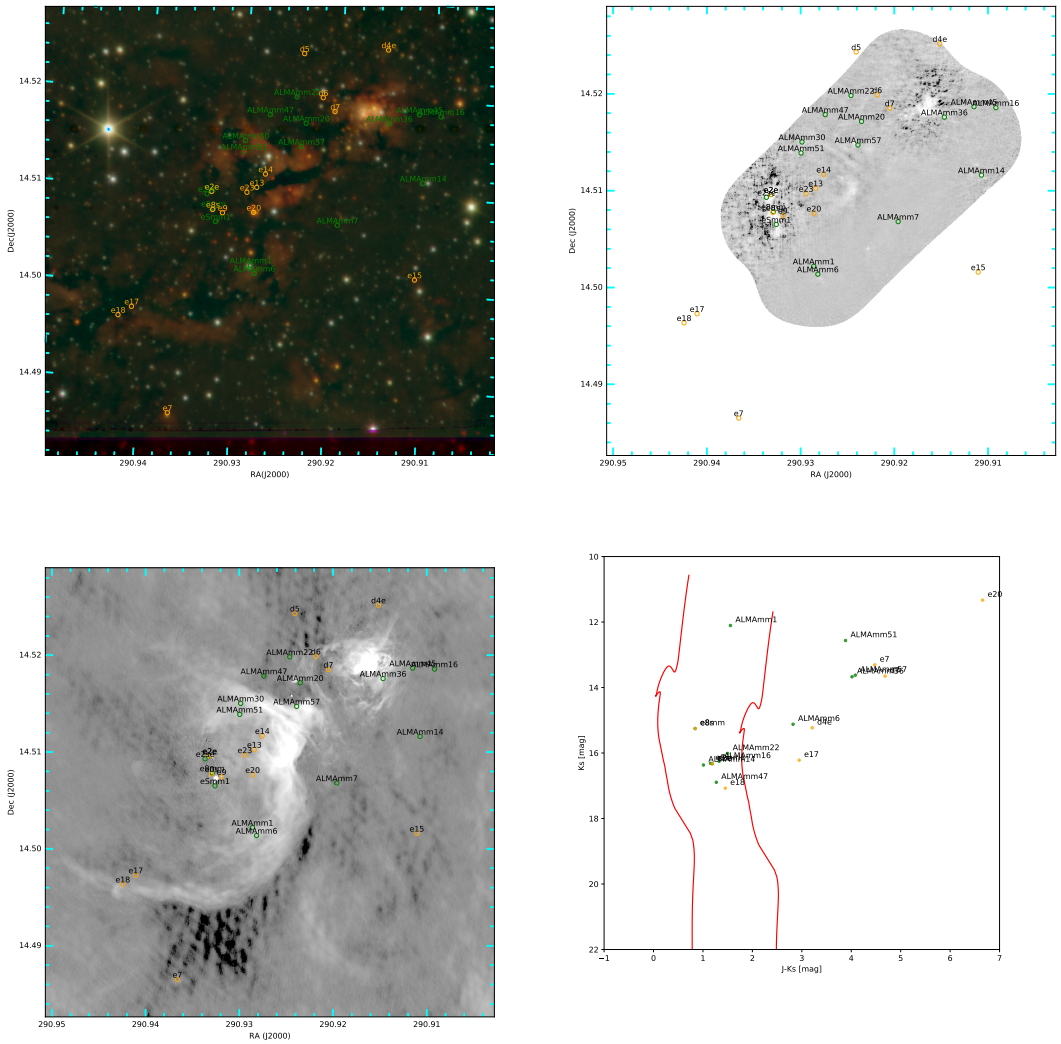

Fig: ALMA/VLA/GTC view of W51A Main. The associated compact source catalogues are almost mutually exclusive. Figure provided by C. Román-Zúñiga.

The Effect of Feedback Appears Insufficient

- At least for some the most massive cluster-forming regions (W49A, W51A), the ionized feedback of tens of forming massive ($M_\star > 20\ M_\odot$) stars **has not yet** significantly disrupted their cloud.
- Yet it is key to regulate accretion and set the SF efficiency (Adam Ginsburg's talk).

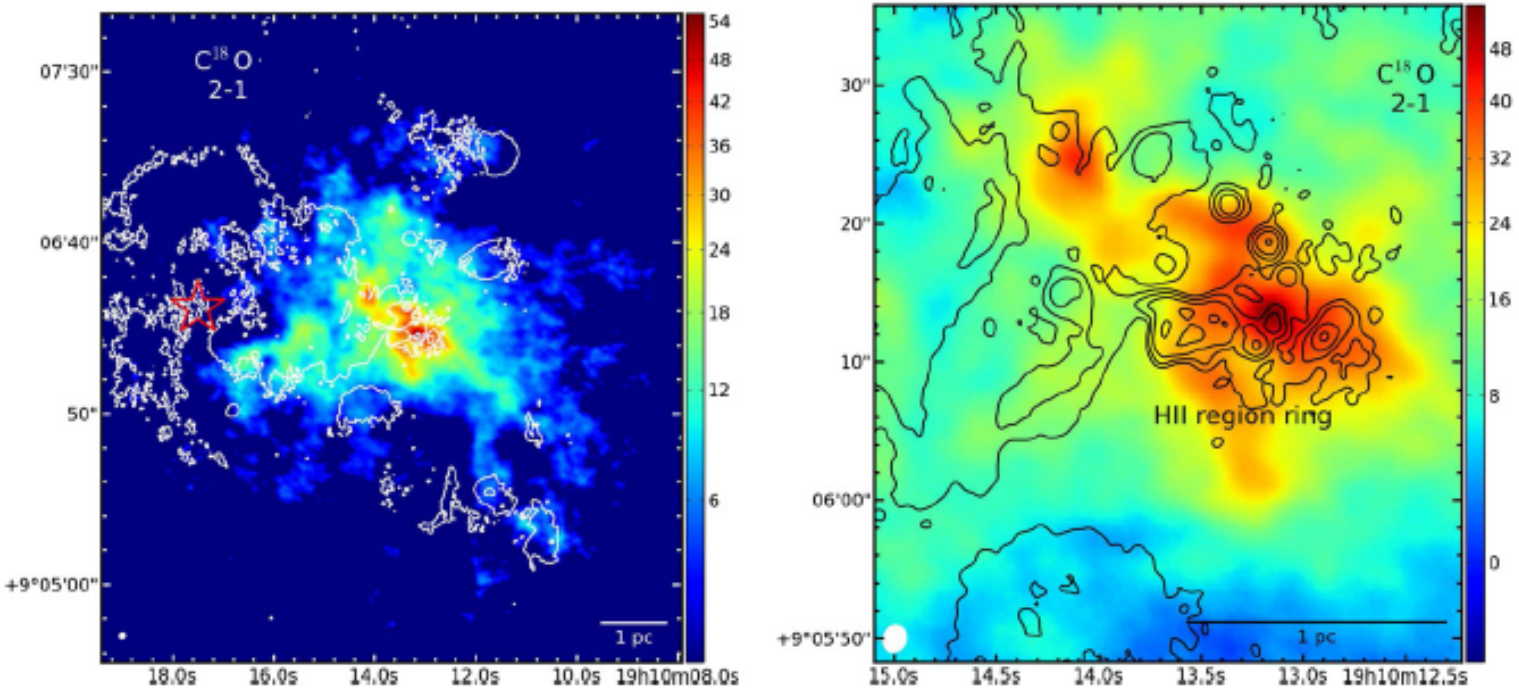

Fig: W49N clump at the center of W49A.Colors: $C^{18}O$ 2–1 velocity-integrated emission. Contours: cm continuum from ionized gas (VLA). Star: NIR cluster (Alves and Homeier 2003).

HC HII Region Quenching in W49N

- HII region quenching due to interaction with molecular accretion flow (Walmsley 95, Peters+2010).
- A 40% flux decrease close to source G2 in the 'Welch' ring at the edges of one of the densest filamentary structures.

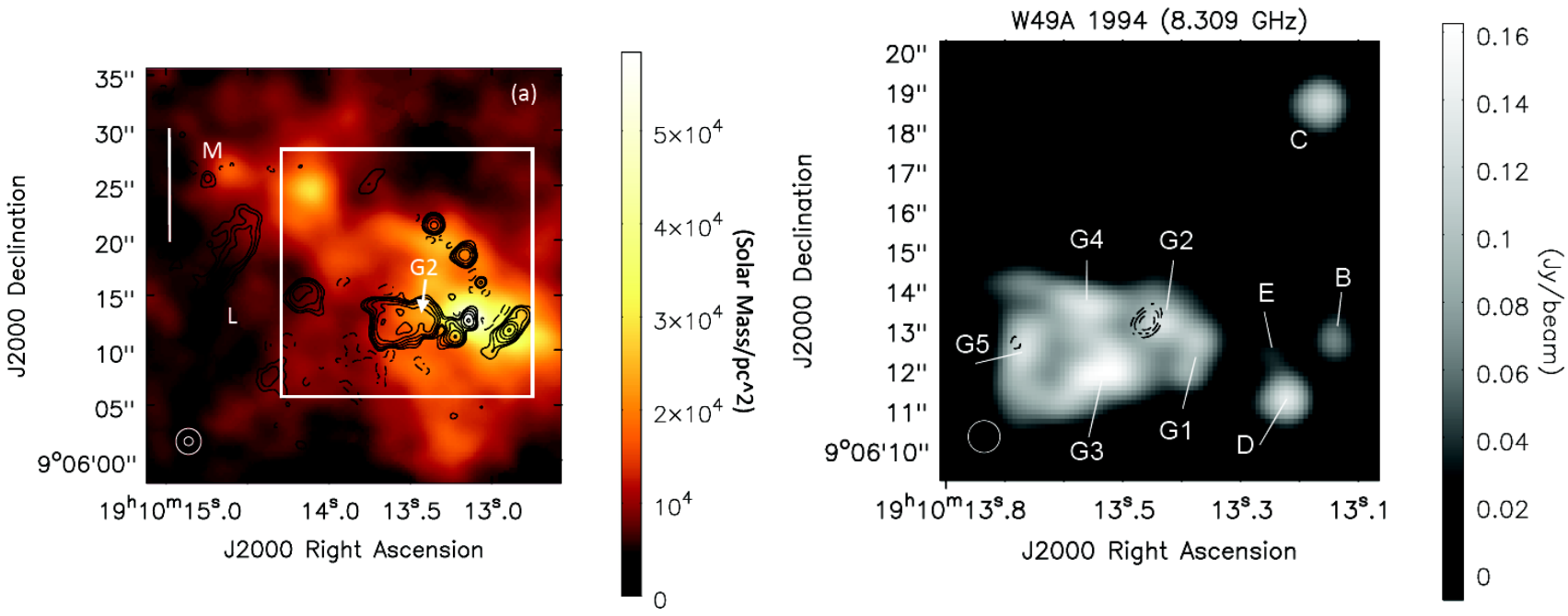

Fig: *Left:* 2015 VLA 3.5-cm image overlaid on column density map. *Right:* 2015-1995 3.5-cm difference (contours) overlaid on 1994 image.
De Pree, G-M, Goss, Klessen et al., submitted.

Asymmetric Accretion in W51

Asymmetric accretion streamers toward candidate ~ 100 au disks around some of the well-known massive protostars in W51 (see Goddi's talk).

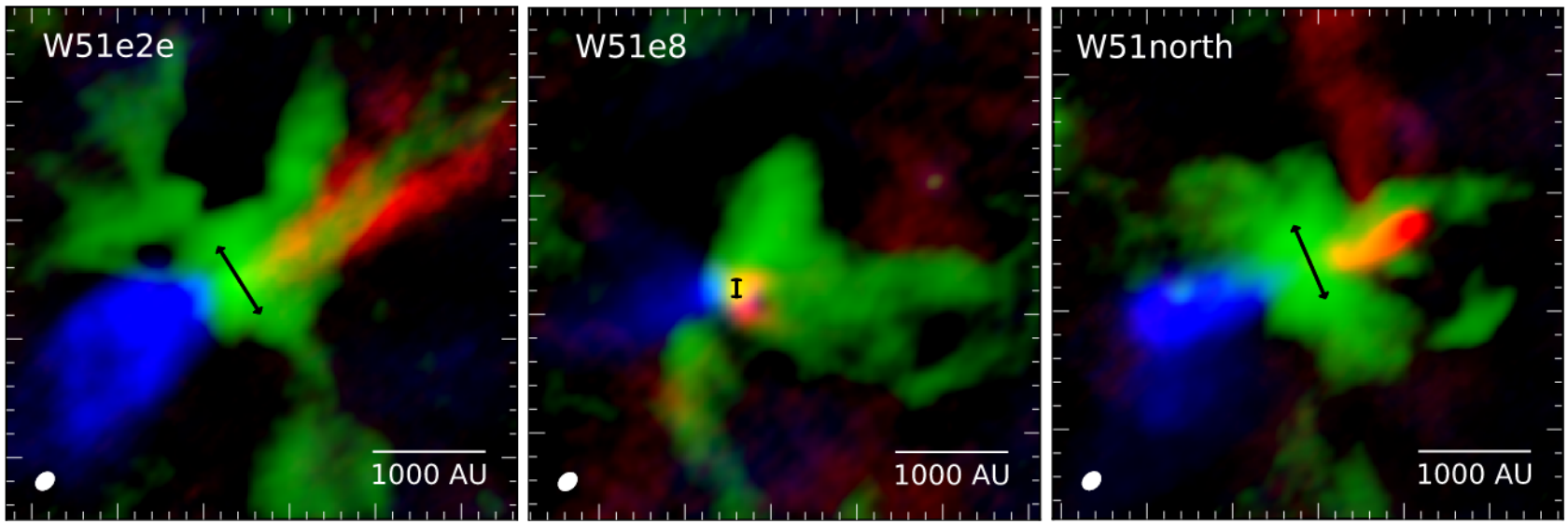

Fig: 1.3 mm (green), SiO (red/blue). From Goddi et al. 2018.

CONCLUSIONS

1) Existence of mass inflows between adjacent scales in the formation of massive star clusters and smaller bound associations.

2) The MW clouds currently forming massive stellar clusters/associations are diverse. Shear and rotation could be the origin of this diversity.

3) Subarcsecond resolution, (sub)mm, cm, and IR observations are needed to build a complete census of the pre-, proto-, and young-stellar populations in massive star clusters in formation.

4) Under some conditions (very large concentrations of stellar/gas masses), feedback from forming massive ($M_\star \sim 10^4\ M_\odot$) stellar clusters appears inefficient to disrupt their parent $M_{\rm gas} \sim 10^5\ M_\odot$ clumps.

Extra Slides

‘SF3dmodels’ Library

https://github.com/andizq/star-forming-regions
Izquierdo et al. 2018, MNRAS

star-forming-regions

About SF3dmodels

SF3dmodels is a star-forming-region(s) modelling package that brings together analytical physical models from different authors (Ulrich, Keto, Pringle, Whitney) to compute density, velocity, temperature, abundance and gas-to-dust ratio 3D distributions.

SF3dmodels makes it possible to construct diverse distributions by mixing the available standard models within it. However, new models can be added to the package if needed. Users willing to contribute and nourish the package with new models are very welcome!

In addition, SF3dmodels can couple different star forming regions together to recreate complex star forming systems as those being revealed by recent telescopes and interferometers. This feature was quite used by Izquierdo et al, 2018 to model the complex star forming system W33A MM1.

We made the SF3dmodels output data to be compatible with LIME: To simulate real observations you need first to perform radiative transfer calculations and LIME does this for you in far-infrared and (sub-)millimeter wavelengths.

Installation process

Download the package folder and place it in your prefered location 📂. Then, modify the Python Module Search Path in your shell startup file as follows:

for Bash shell (sh):

In your startup file (`~/.bash_profile` , `~/.bash_login` or `~/.bashrc` [Linux users], and `~/.profile` [Mac OS users]) include:

```
export PYTHONPATH=${PYTHONPATH}:/path/to/package
```

for C Shell (csh; tcsh):

In your startup file (`~/.cshrc` , `~/.tcshrc` or `~/.login`) include:

```
setenv PYTHONPATH $PYTHONPATH\:/path/to/package
```

‘SF3dmodels’ Library

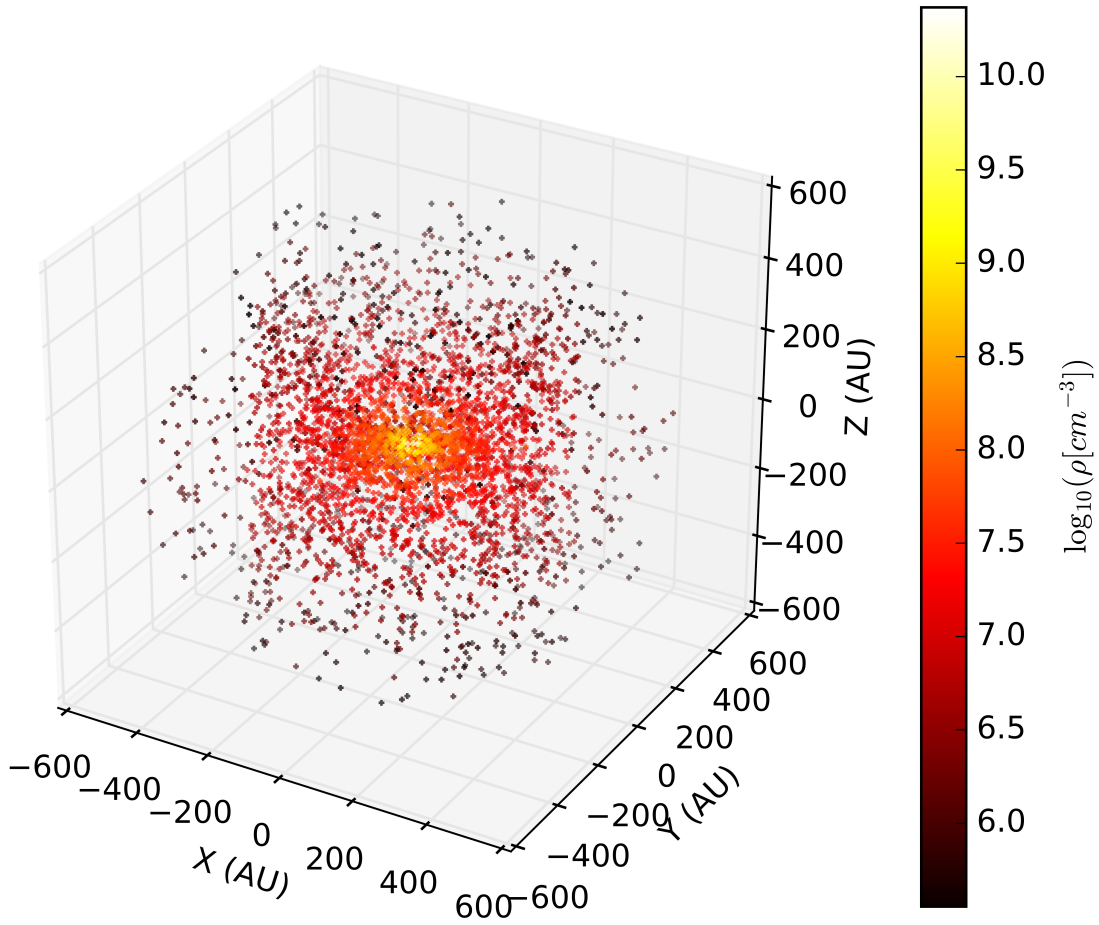

Local grids.

‘SF3dmodels’ Library

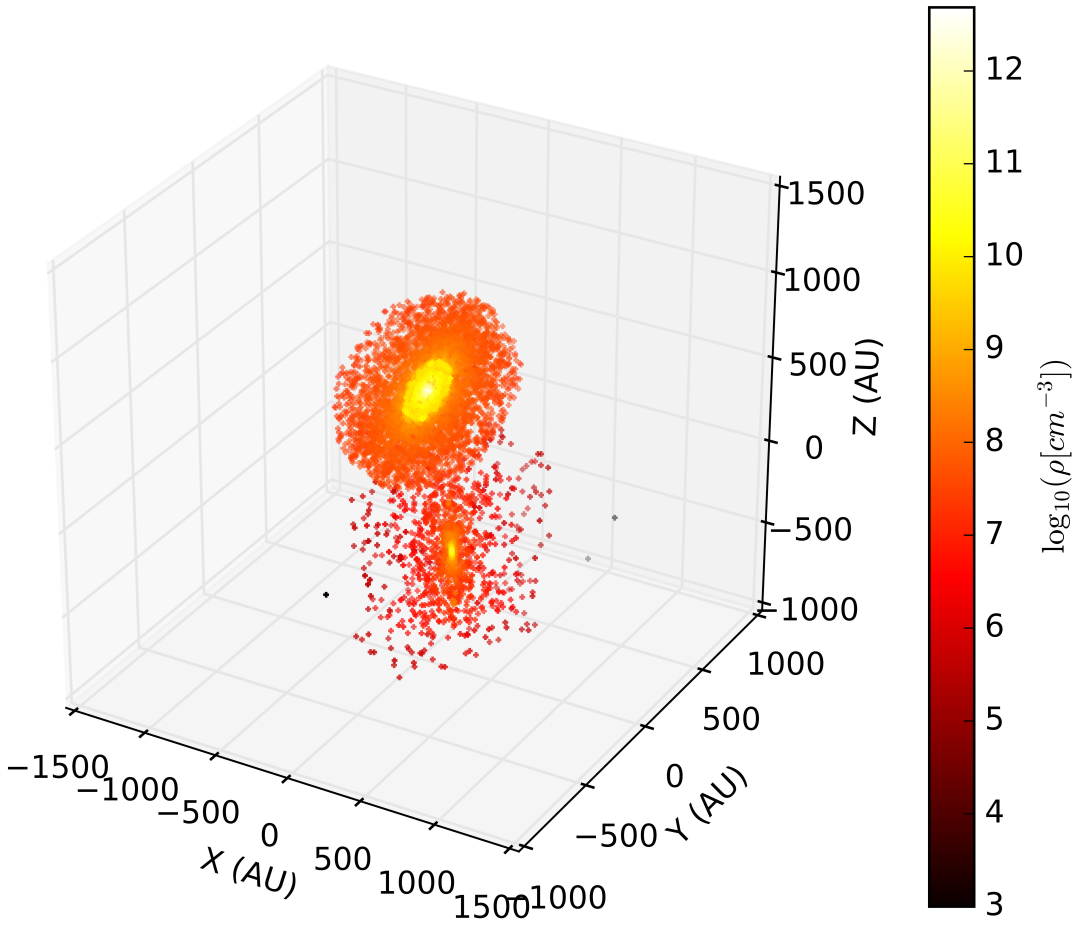

Global grids.

‘SF3dmodels’ Library and Digestors

Tested Features

- Current model grids: disks (Pringle, w/o holes and rings), envelopes (Ulrich-Mendoza, turbulent sphere), filaments (cylindrical or parabolic, w/o density and velocity gradients).
- Other features: Co-adding of ‘local grids’ into a ‘global grid’ (e.g., 3 disks+envelopes, 2 envelopes, 5 filaments), with their rotation, translation, Doppler shift, and overlap ‘properly’ taken into account.
- Digestor of cartesian model grid into LIME’s random-like grid. LIME calculates the radiation transport of dust continuum and molecular line emission across the model, Brinch & Hogerheijde 2010).

'SF3dmodels' Library and Digestors

Tested Features

- Current model grids: disks (Pringle, w/o holes and rings), envelopes (Ulrich-Mendoza, turbulent sphere), filaments (cylindrical or parabolic, w/o density and velocity gradients).
- Other features: Co-adding of 'local grids' into a 'global grid' (e.g., 3 disks+envelopes, 2 envelopes, 5 filaments), with their rotation, translation, Doppler shift, and overlap 'properly' taken into account.
- Digestor of cartesian model grid into LIME's random-like grid. LIME calculates the radiation transport of dust continuum and molecular line emission across the model, Brinch & Hogerheijde 2010).

New Features (2018)

- Digestor into RADMC3D (Dullemond).
- Free-free and radio recombination line model library: jets (Reynolds model, w/o truncation), photoevaporating flow from disk (Hollenbach), UC/HC HIIs (spherical w/o gradients, bipolar), Keto HII region (accreting inside r_g, outward flow outside), ionized Pringle disk (can that exist?).

What we learned from the W33A MM1 core?

An accretion filament feeding the fragmented high-mass core W33A MM1

- $M_{\rm gas} \sim 0.4\ M_\odot$, $\dot{M} \sim 5 \times 10^{-5}\ M_\odot\ {\rm yr}^{-1}$, $l \sim 7300$ au.
- Replenishment from larger scales suggested from observations (G-M + 2010, Maud + in prep.) and from ~ 8000 yr duty cycle.

Accretion filaments joining pairs of protostars

- The existence of 3 of the 5 proposed is robust but their implementation as straight cylinders is questionable.
- Their combined mass-flow rate adds to $\dot{M} \sim 4 \times 10^{-5}\ M_\odot\ {\rm yr}^{-1}$, dominated by flows to Main and MNE and close to the 'total' inflow rate (as determined by the larger 'core-feeding' filament).

CURRENT: VELOCITY STRUCTURE

- The kinematics in the central few pc is more complex.

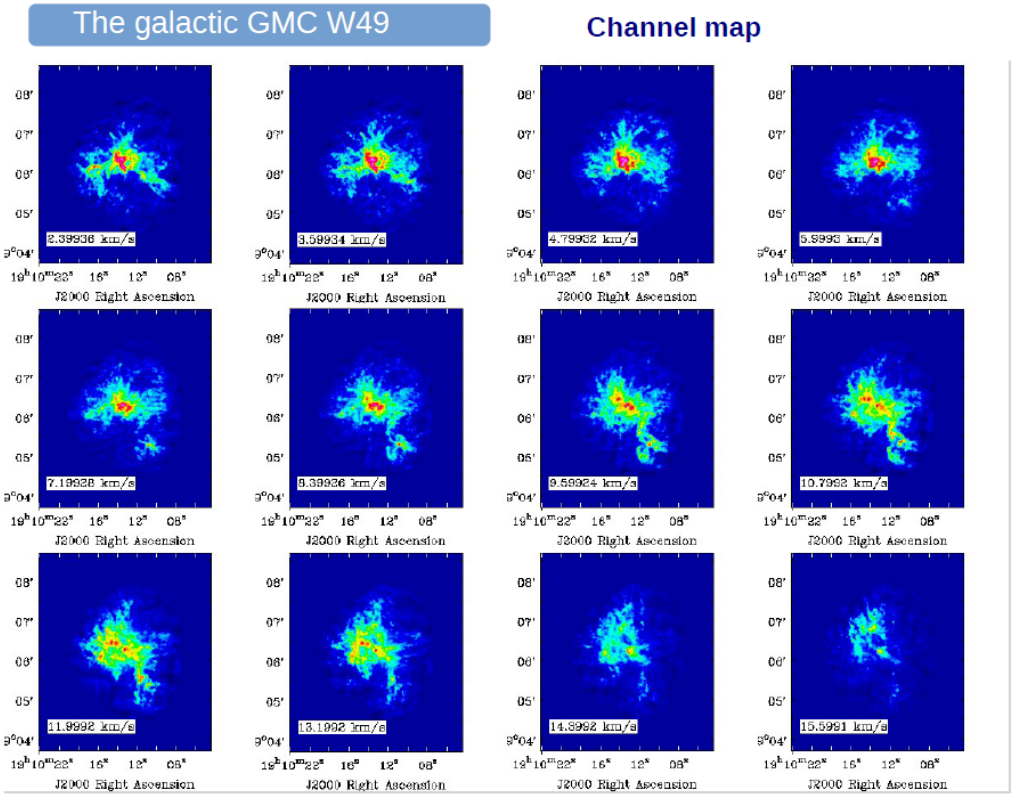

^{13}CO 2–1 SMA+IRAM 30m data.

CURRENT: VELOCITY STRUCTURE

- The kinematics in the central few pc is more complex.

The galactic GMC W49

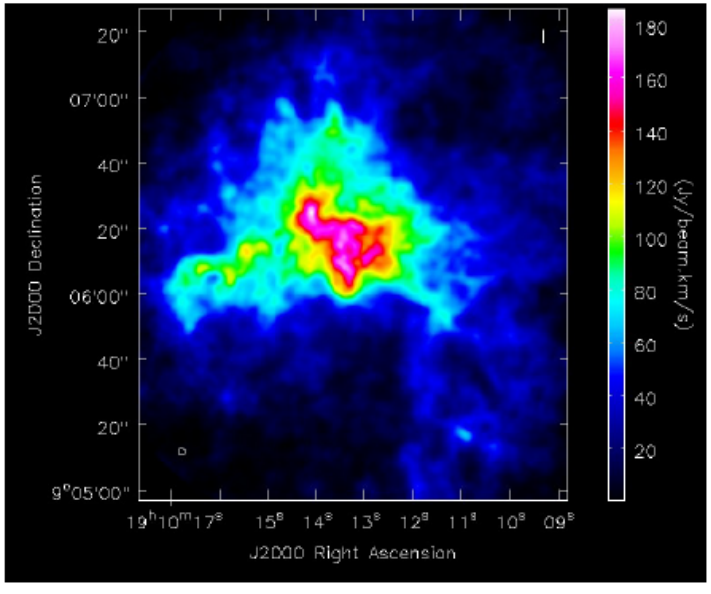

Integrated intensity map

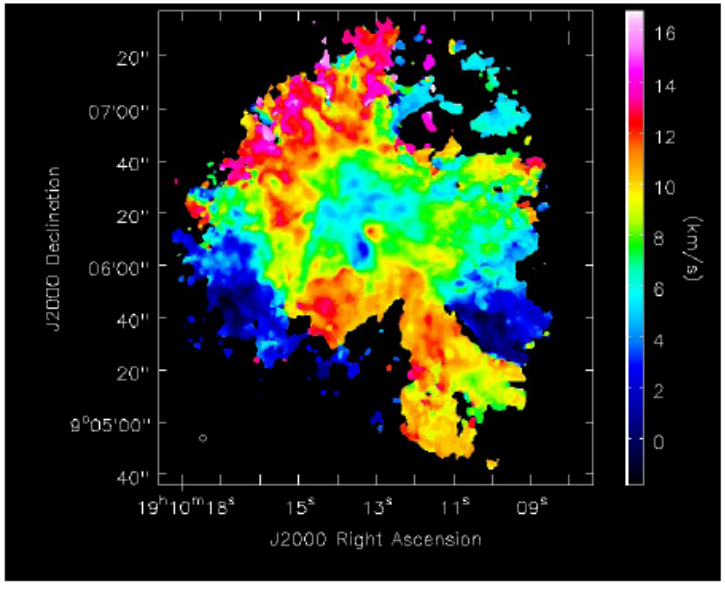

Velocity intensity map

^{13}CO 2–1 SMA+IRAM 30m data.

CURRENT: SPECTRAL CORRELATION FUNCTION

The spectral correlation function (SCF, Rosolowsky+99, Padoan+01) can be used to discriminate physical models of GMCs.

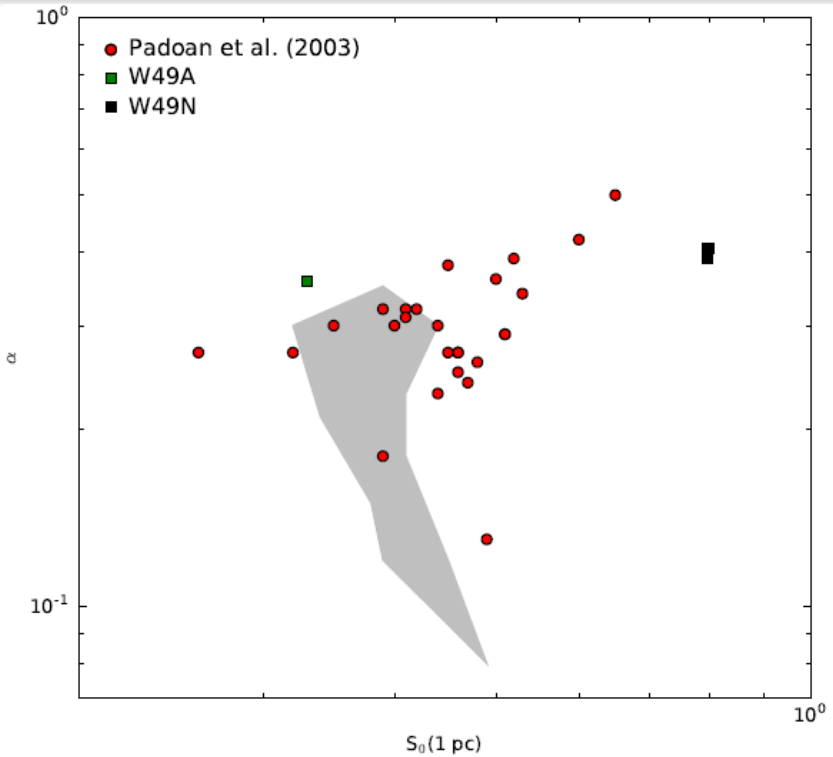

Fig: SCF at 1 pc vs slope for W49A (full GMC), W49N (starbursting region), other MW clouds (red points), and turbulent-box models (gray, Padoan+). Pineda, G-M, Liu et al. in prep.

CURRENT: SPECTRAL CORRELATION FUNCTION

- The central starburst (W49N) is way off other MW clouds and turbulent box models.
- Pure turbulence is not enough. Gravity?

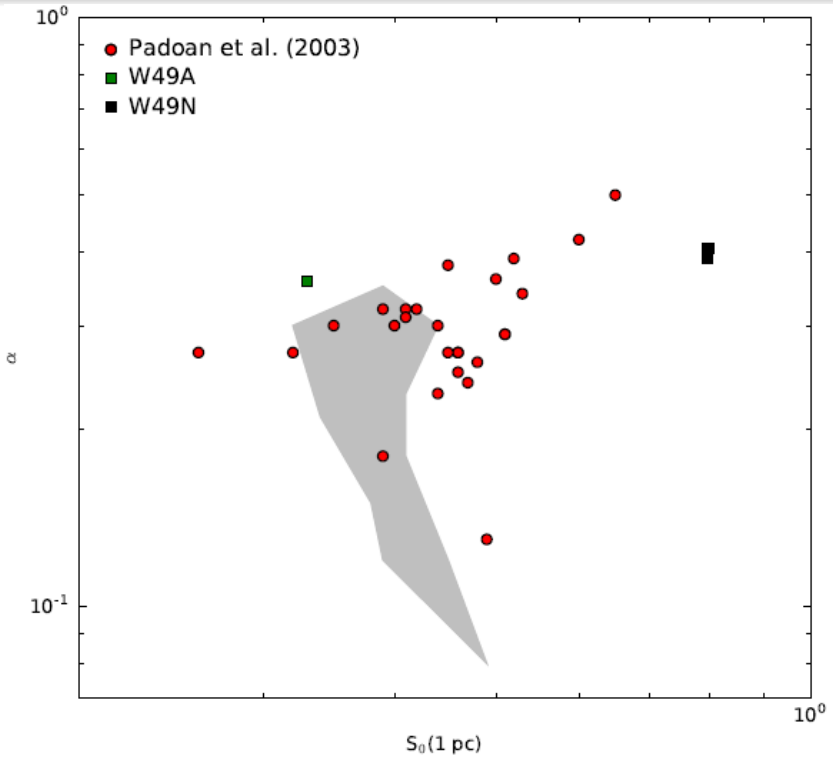

Fig: SCF at 1 pc vs slope for W49A (full GMC), W49N (starbursting region), other MW clouds (red points), and turbulent-box models (gray, Padoan+). Pineda, G-M, Liu et al. in prep.

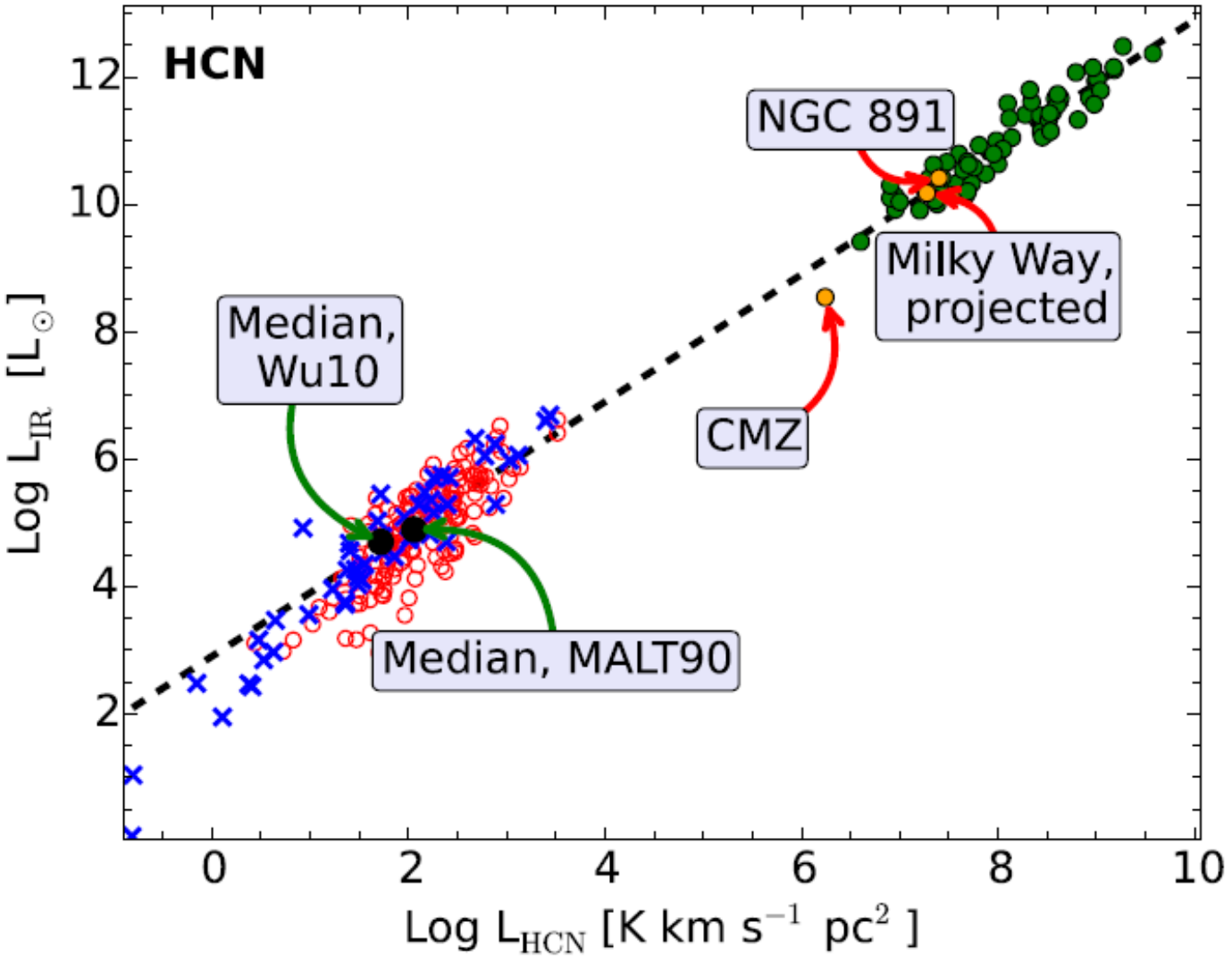
HCN
NGC 891
Milky Way,
projected
CMZ
Median,
Wu10
Median, MALT90
Log L_IR [L_⊙]
Log L_HCN [K km s^-1 pc^2]
12
10
8
6
4
2
0
2
4
6
8
10

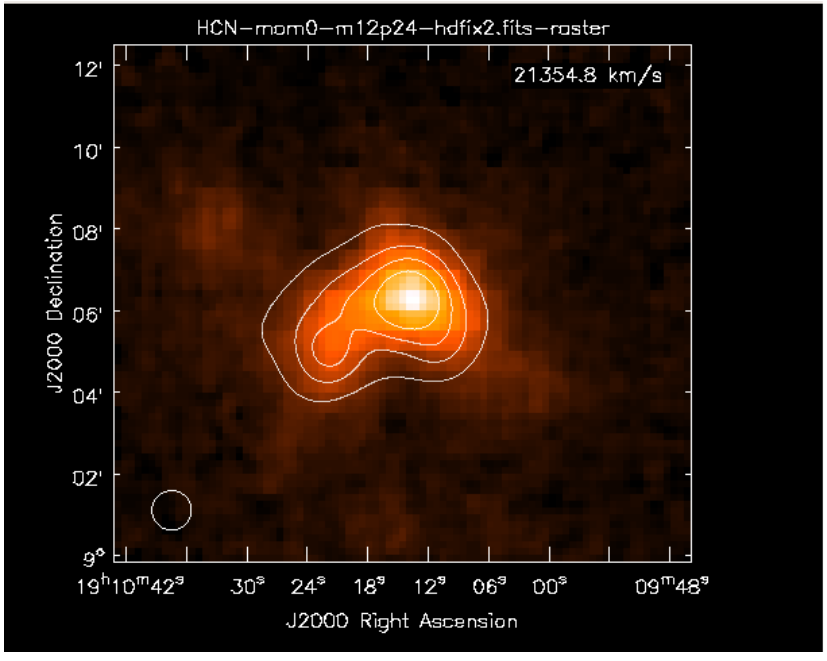
HCN−mom0−m12p24−hdfix2.fits−raster
21354.8 km/s
12'
10'
08'
06'
04'
02'
9°
J2000 Declination
19h10m42s
30s
24s
18s
12s
06s
00s
09m48s
J2000 Right Ascension

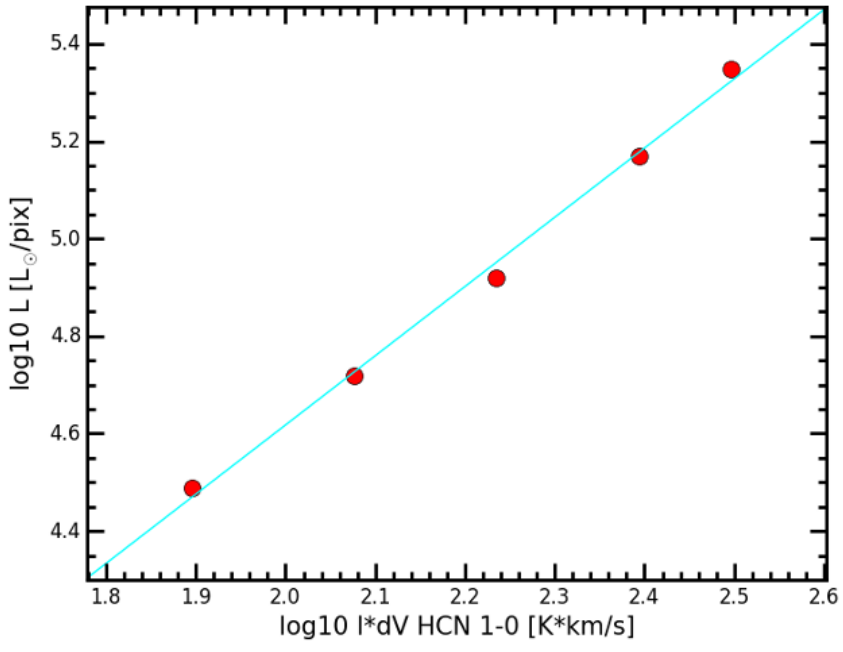
5.4
5.2
5.0
4.8
4.6
4.4
log10 L [L⊙/pix]
1.8
1.9
2.0
2.1
2.2
2.3
2.4
2.5
2.6
log10 I*dV HCN 1-0 [K*km/s]

CURRENT PROJECTS: LMT/AzTEC 1 mm MAPPING

- LMT/AzTEC maps already better than previous CSO-BOLOCAM and could get $\times 3$ deeper.
- Combine them with SMA mosaic to obtain core mass function in starburst regime.

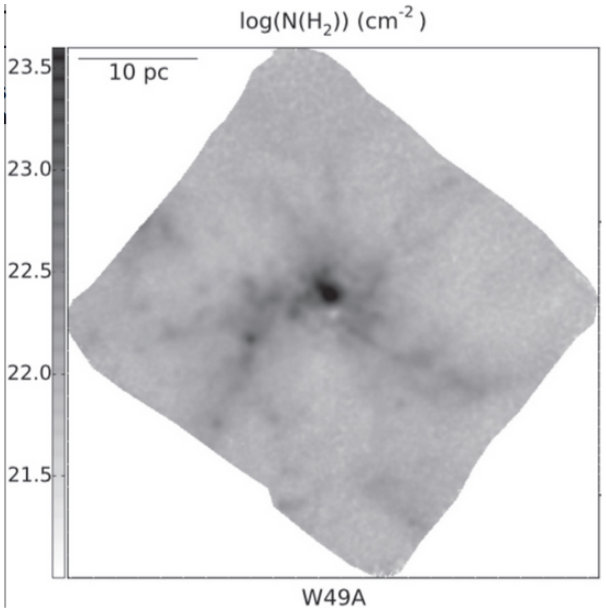

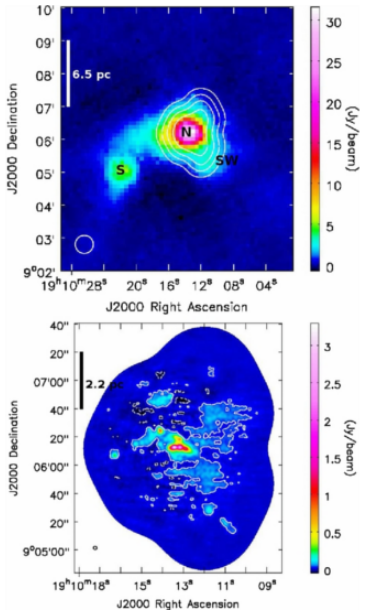

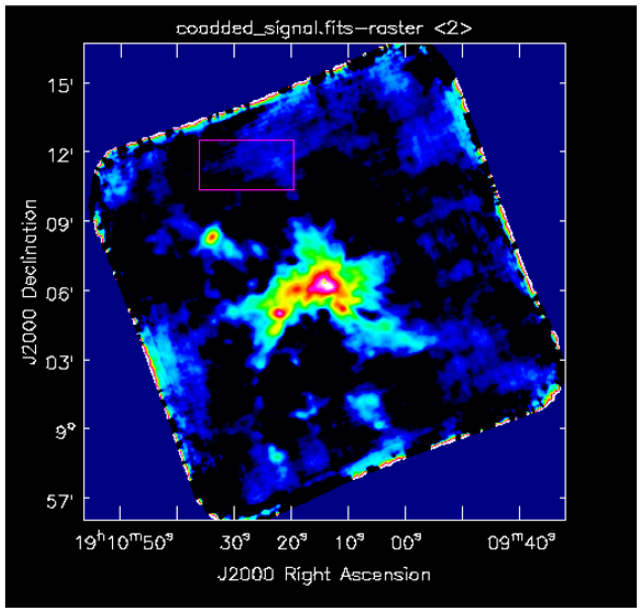

Right: column density map from Lin+2016. Center: previous combination of CSO/BOLOCAM with SMA from G-M+2013. Right: new LMT data.

OB Cluster-Forming Molecular Hub-Filament System

An extremely rich astrophysical problem

On the Large Scale

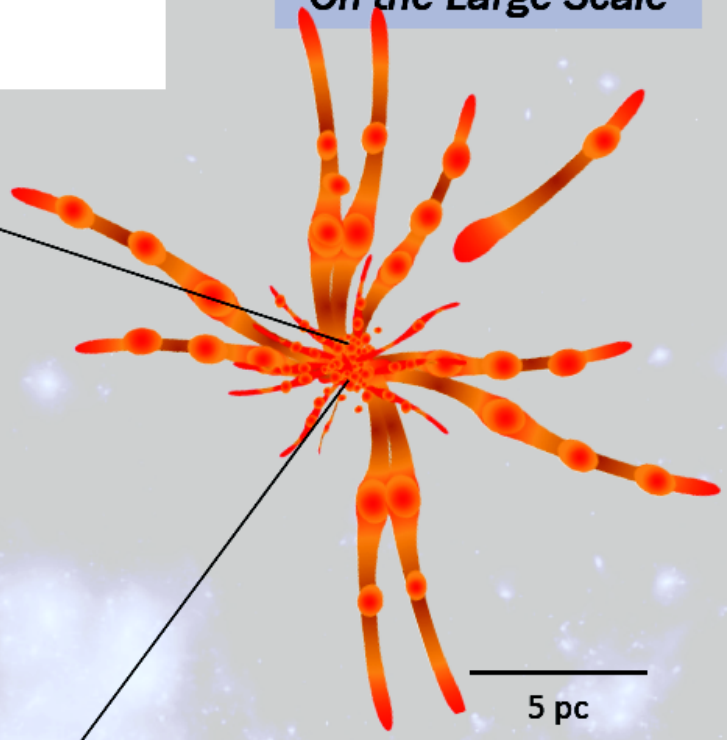

Within the Centrifugal Radius

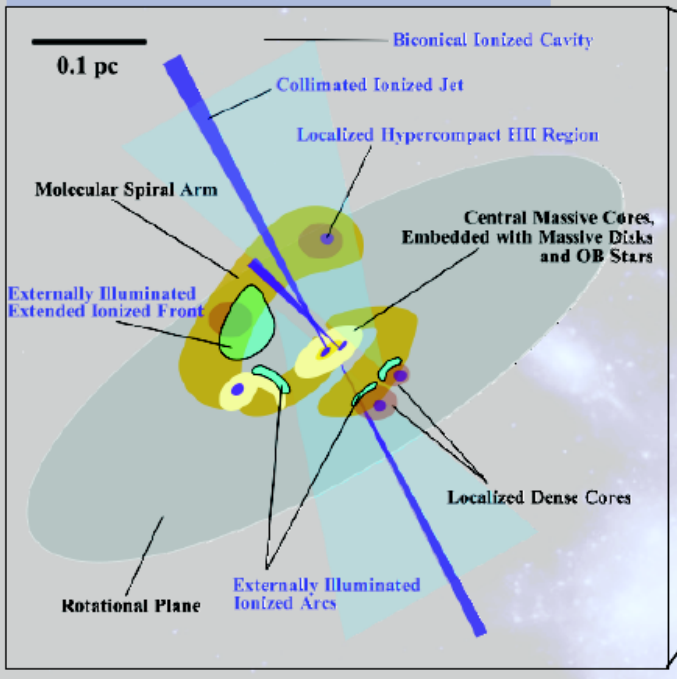

2014.December.11 Tokyo ALMA Conf.

Current: mm recombination lines

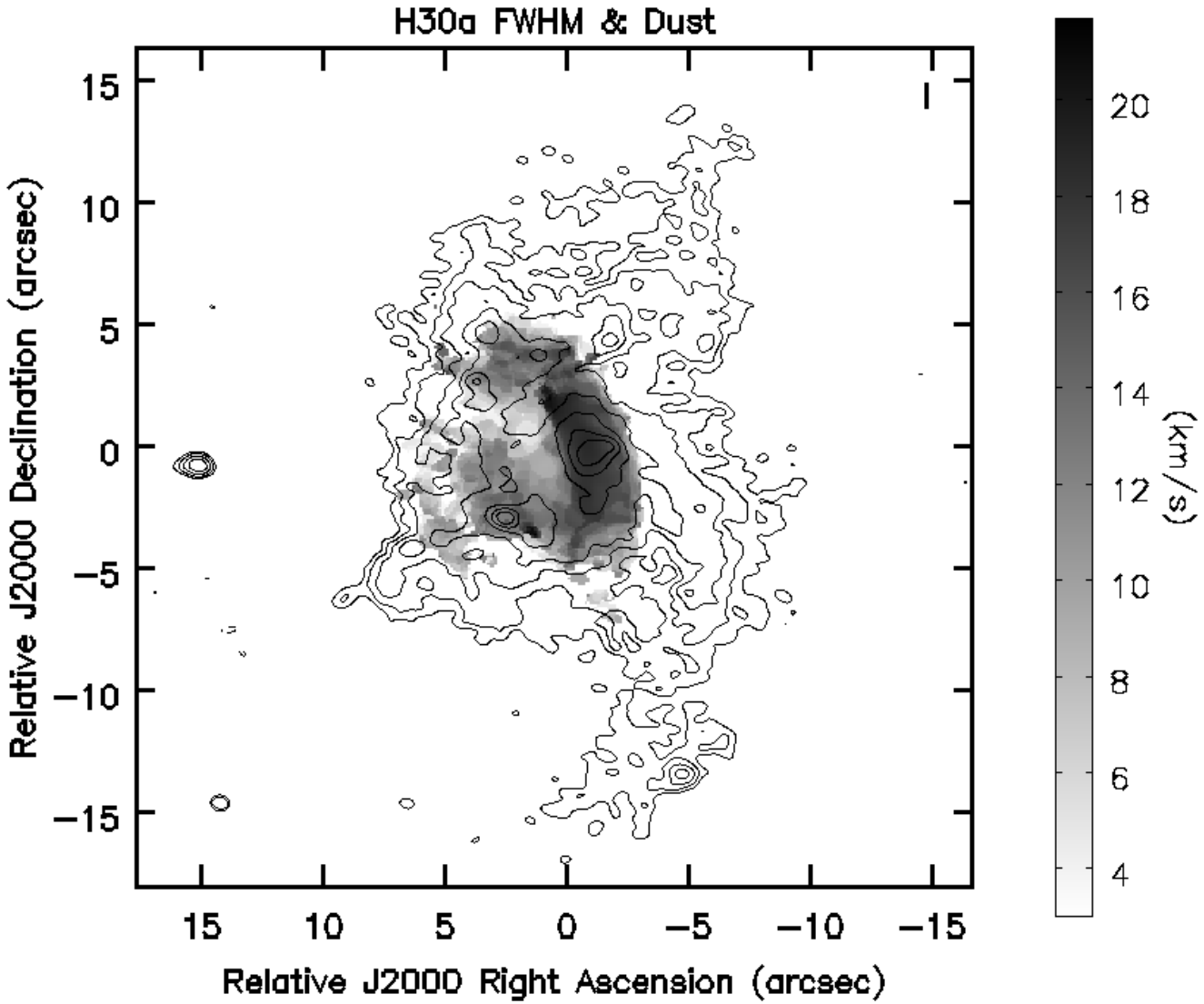

Fig: H30α and He30α recombination line study. Hernández-Hernández, G-M, Tafoya+, in prep.

Current: mm recombination lines

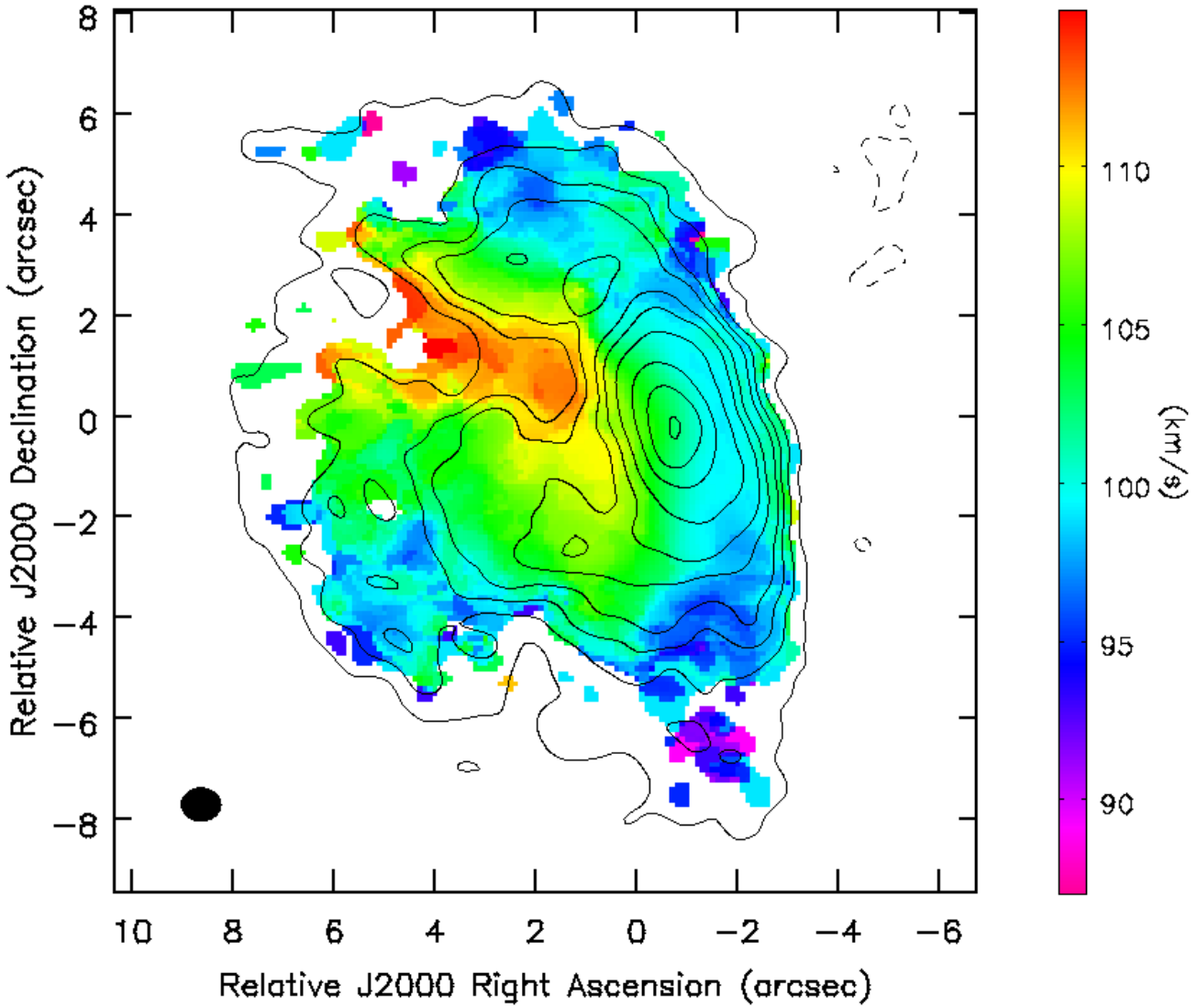

Fig: H30α and He30α recombination line study. Hernández-Hernández, G-M, Tafoya+, in prep.

Current: mm recombination lines

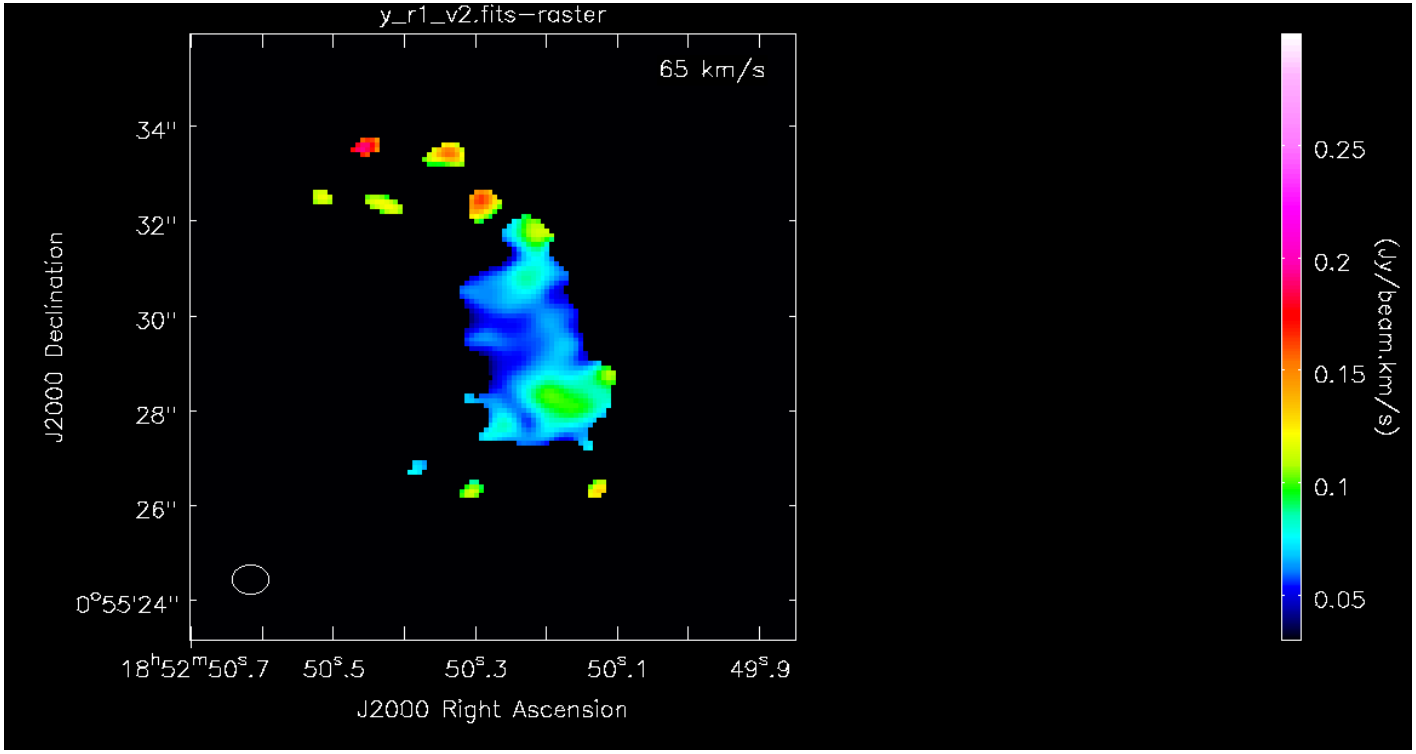

Fig: H30α and He30α recombination line study. Hernández-Hernández, G-M, Tafoya+, in prep.

Velocity Field in G33

- Face-on system: great for morphology, bad for kinematics
- Channel width for DCN 3–2 and ^{13}CS 5–4 is 0.7 km/s $\Rightarrow$ few channels per linewidth
- Evidence of velocity gradient between two main arms

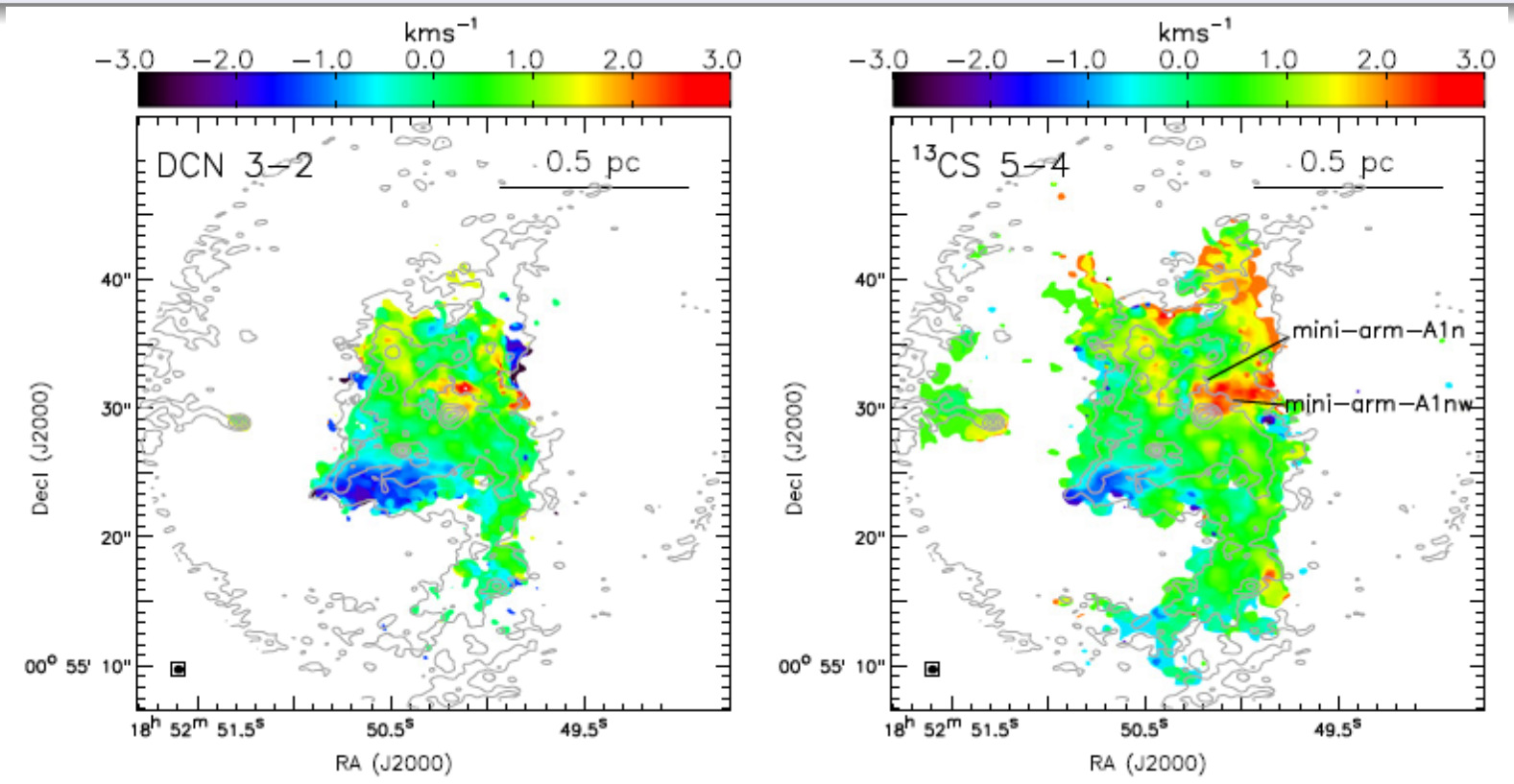

Fig: Intensity-weighthed mean velocity (colors) and dust continuum (contours)

Spirals Everywhere

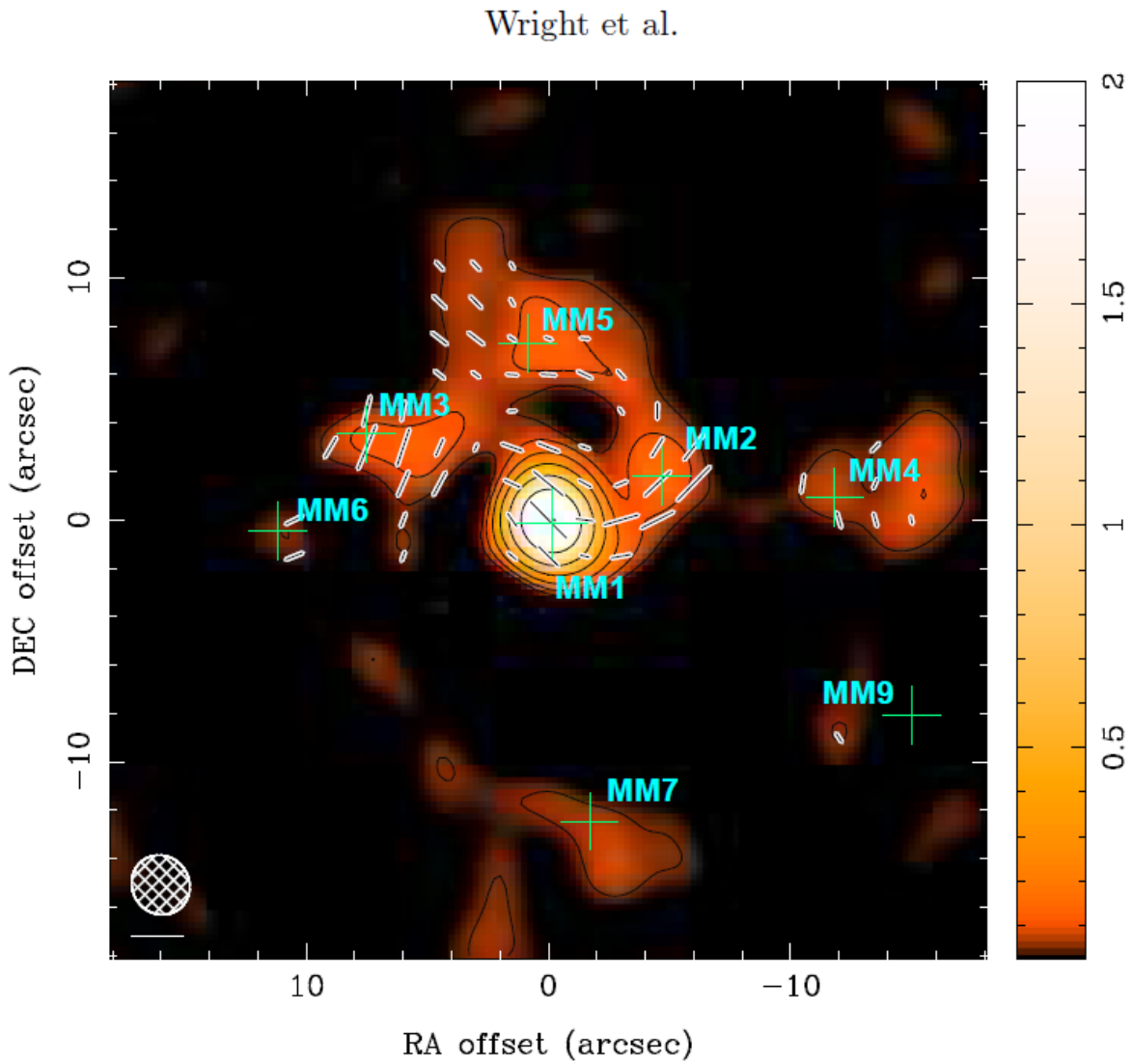

Fig: Polarized dust spiral in the NGC 7538 luminous ($L \sim 10^5\ L_\odot$) star forming region (Wright+2015).

Lin+2016 Data and Algorithm

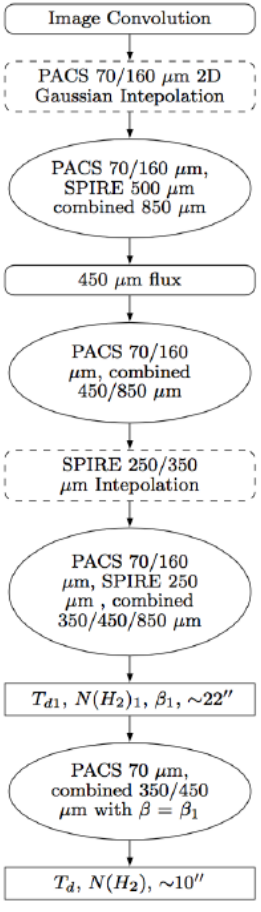

FIG. 1.— The image combination and SED fitting procedure, including the iterative processes to derive the saturated pixels or interpolate the corresponding space telescope image for several wavelengths observations. Each ellipse in the flow chart represents a SED fitting process. For more description see Section 2.4.

Lin+2016 Data and Algorithm

TABLE 2
OBSERVATIONAL PARAMETERS OF MULTI-BAND DATA

λ (μm) Camera	Beam *FWHM* (arcsec)	Pixel size (arcsec)	Flux unit
70/PACS	5.8×12.1	3.2	Jy/pixel
160/PACS	11.4×13.4	3.2	Jy/pixel
250/SPIRE	18.1	6.0	MJy/sr
350/SPIRE	25.2	9.72	MJy/sr
500/SPIRE	36.9	14.0	MJy/sr
450/SCUBA2	8.0	3.0	mJy/$arcsec^2$
850/SCUBA2	14.0	3.0	mJy/$arcsec^2$
350/SHARC2	8.0	1.5	Jy/beam
870/LABOCA	19.2	6.0	Jy/beam
1200/MAMBO-2	11.0	3.50	mJy/beam
217GHz/PLANCK	292.2	60.0	K_{cmb}
353GHz/PLANCK	279.0	60.0	K_{cmb}

CURRENT PROJECTS

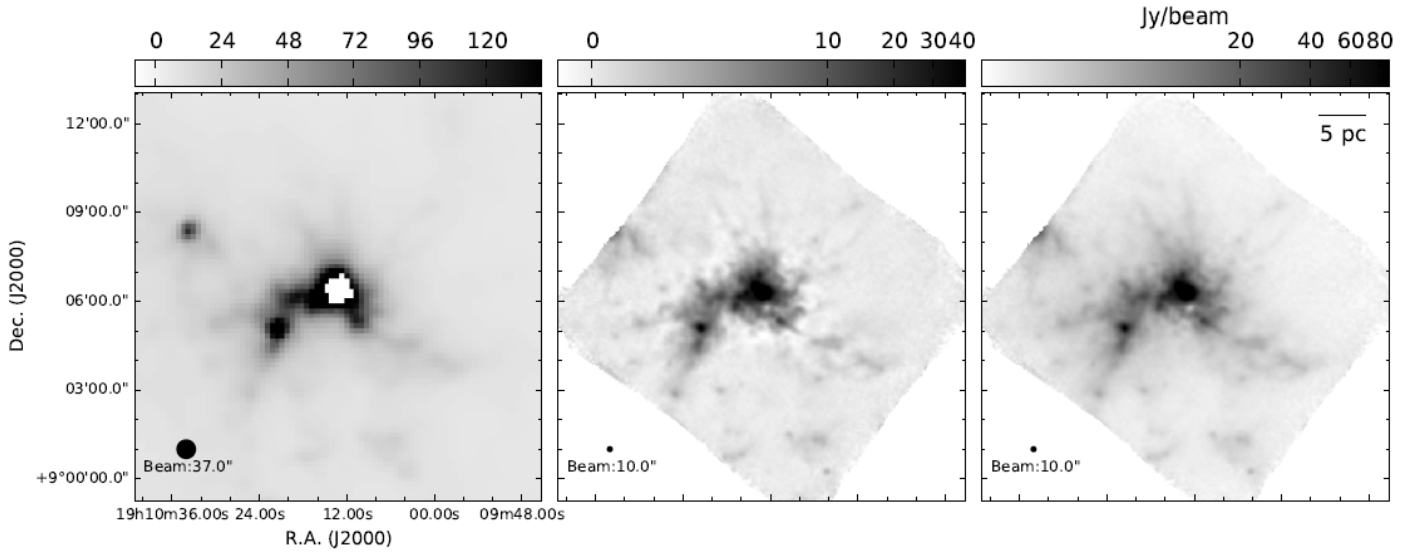

FIG. 2.— The 350 μm image of the W49N mini starburst region, from left to right, SPIRE 350 μm image, SHARC2 350 μm image and image generated by combining the CSO-SHARC2 image with the Herschel-SPIRE image. Color scale for the the middle and right images are stretched to illustrate the difference between the original SHARC2 map with the combined image.

Fig: Herschel SPIRE and CSO SHARC2 350 μm combination in W49A (Lin+2016).

CURRENT PROJECTS

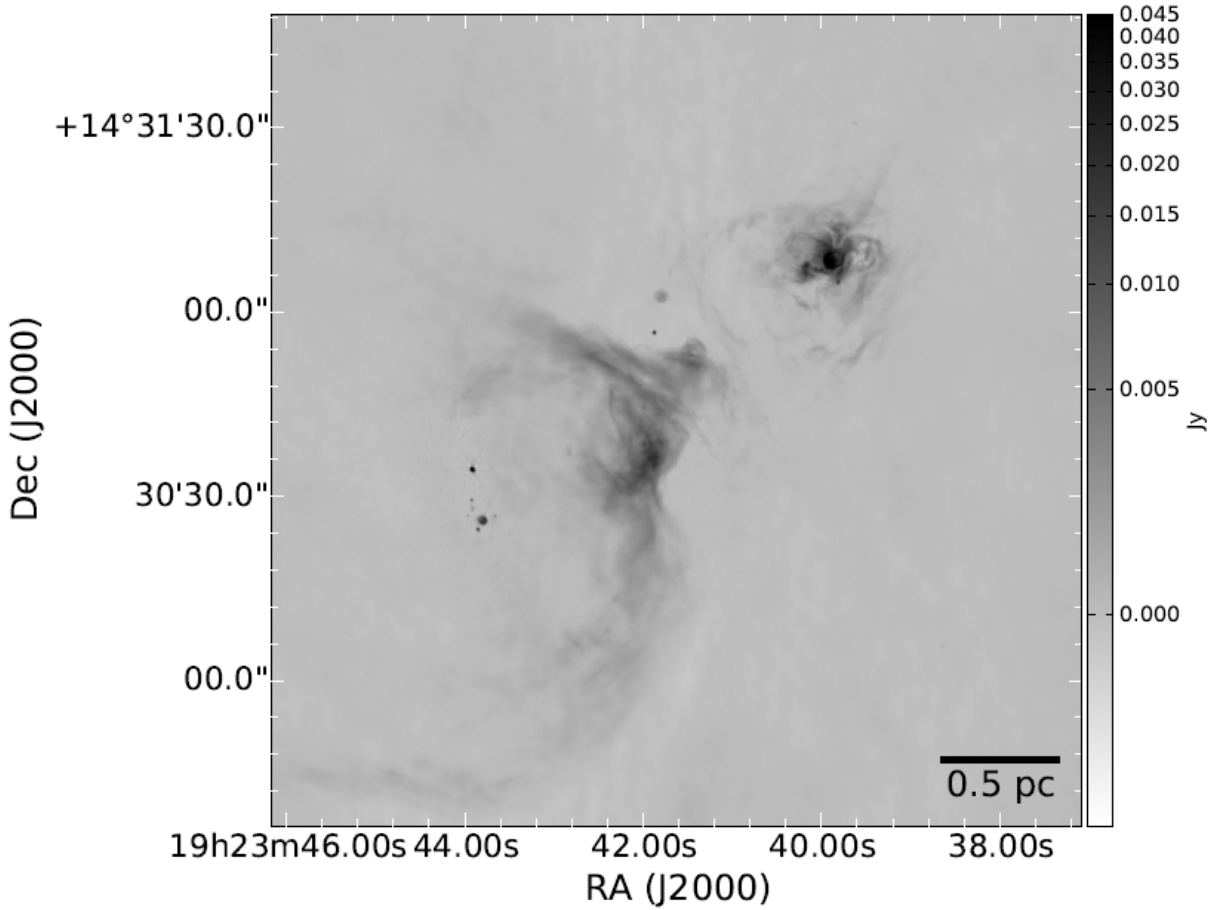

Fig. 1. *K*u-band image (14.5 GHz, tracing ionized gas) of the W51 region produced with a combination of JVLA B and D array data using uniform weighting. The synthesized beam size is $\theta_{\rm FWHM} \approx 0.33''$. The compact, circular region in the upper-right corner is IRS2, while the more diffuse bright region in the center is IRS1, marking the edge of the W51 Main shell. Compact sources are identified in Fig. 2.

Fig: W51A VLA and ALMA (Ginsburg+2016,2017).

CURRENT PROJECTS

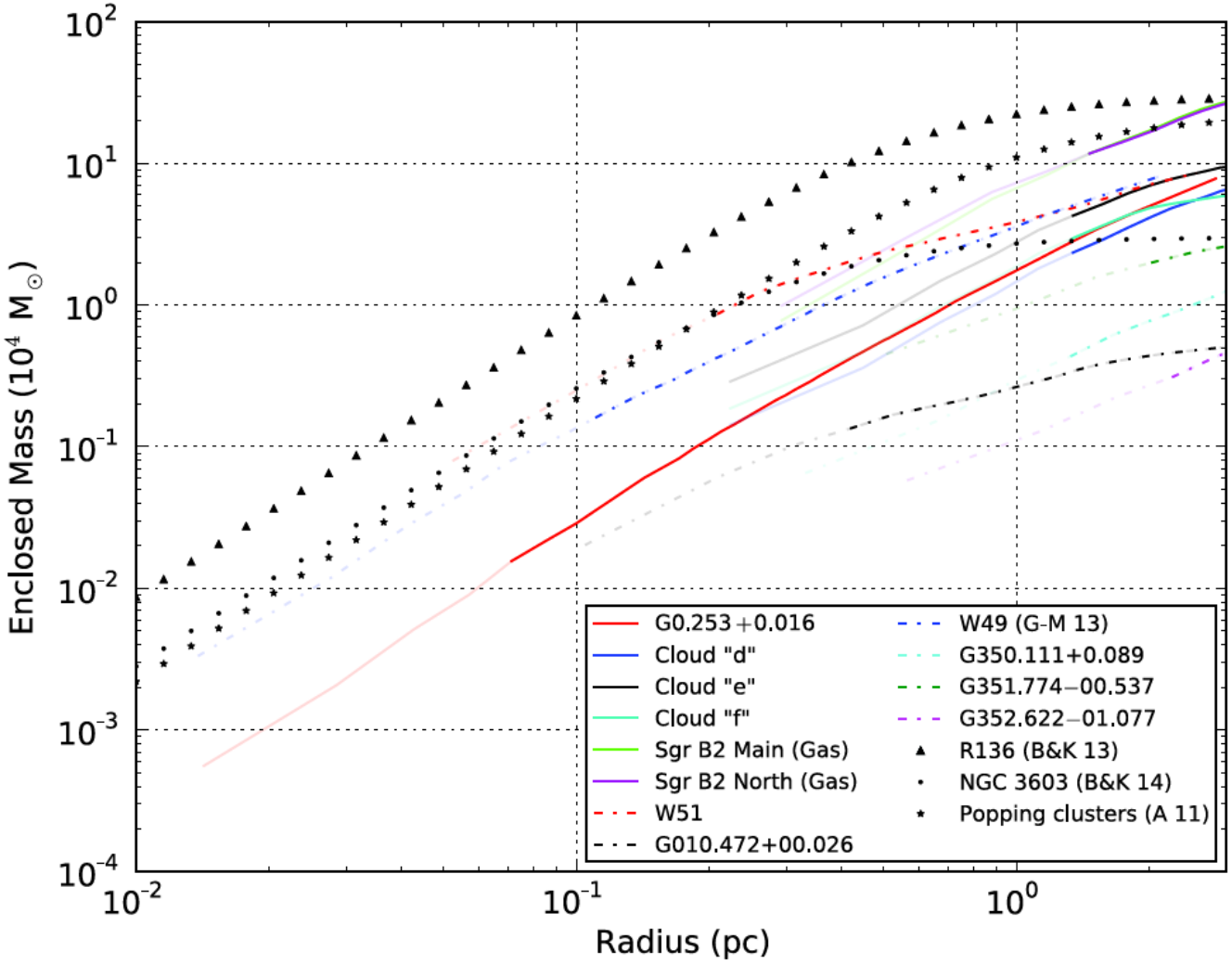

Fig: Comparison of mass profiles of YMC forming clouds (Walker+2016).